

## Spectral properties of the Hubbard bands

Henk Eskes

*Max-Planck-Institut für Festkörperforschung, Heisenbergstraße 1, D-70569 Stuttgart, Federal Republic of Germany*

Andrzej M. Oleś

*Institute of Physics, Jagellonian University, Reymonta 4, PL-30059 Kraków, Poland*

Marcel B.J. Meinders

*Applied and Solid State Physics, University of Groningen, Nijenborgh 4, NL-9747 AG Groningen, The Netherlands*

Walter Stephan

*King's College London, Strand, London WC2R 2LS, United Kingdom*

(Received 7 June 1994)

Using strong-coupling perturbation theory for the Hubbard model, explicit expressions are obtained for the integrated weights, energy positions, and widths of the upper and lower Hubbard bands separately, both for the optical and photoemission spectrum. In one dimension all expressions can be explicitly evaluated using the large- $U$  Bethe-ansatz wave function. The  $\vec{k}$ -dependent moments for the one-particle spectrum are compared with the closely related two-pole ansatz. The strong momentum dependence of the spectra demonstrates the importance of the  $\vec{k}$ -dependent correlation functions in the spectral moments, which are often neglected. In order to estimate corrections due to the neglect of higher-order terms (in  $t/U$ ), all results are compared with numerical-diagonalization data for intermediate- $U$  values. The sum-rule results show a rapid spectral-weight transfer from the high- to the low-energy regime upon doping, similar to what is observed experimentally in one-particle and optical spectra of Cu (high- $T_c$ ) and Ni compounds. Such fast weight redistributions as a function of the carrier density are a natural consequence of the strong correlations in these materials. The redistribution of intensity in the optical conductivity is connected with the dilution of the spin system by the added holes. For the one-particle spectrum the decrease of weight in the upper Hubbard band away from half filling can be understood by state counting at  $U = \infty$ , and the effect is strongly enhanced for small doping by both the first- and second-order terms in  $t/U$ . Altogether, the one-particle and optical spectra show the importance of the three-site hopping term. Therefore the  $t$ - $J$  model does not represent well the spectral properties of the Hubbard model at large  $U$ . The local spin order is essential and determines both the  $\vec{k}$  dependence of the one-particle spectrum and the intensities in the optical spectrum.

### I. INTRODUCTION

The study of the one-band Hubbard model is of general importance since it is one of the simplest models for interacting electrons and because the understanding of correlated systems is still far from complete. After the discovery of the high-temperature superconductors the interest in this model increased greatly. The electronic structure of the  $\text{CuO}_2$  planes resembles the spectroscopic properties of a two-dimensional (2D) square-lattice Hubbard model. At the same time the correlations are strong and are responsible for the vast amount of anomalous (low-energy) normal-state properties observed in these materials.

However, not only the low-energy but also the high-energy ( $\sim$  eV) electronic excitations in these materials show anomalous behavior. This is dramatically demonstrated in particular in the optical conductivity and in the oxygen 1s x-ray-absorption spectroscopy (XAS) experiments or electron-energy-loss spectroscopy (EELS) ex-

periments. In this paper we will demonstrate that these effects can be understood in a generic way as being a consequence of correlations.

In the O 1s EELS or XAS experiments an electron is promoted from the 1s core level to unoccupied levels in the valence band. Therefore this experiment is related to the electron-addition spectrum and the one-particle Green's function. Because of the strong correlations, the undoped  $\text{Cu}^{2+} d^9$  compounds are insulating and the XAS spectrum shows a low-energy peak which can be identified as the upper Hubbard band. When introducing holes (with a concentration  $x$ ), the chemical potential moves into the lower Hubbard band and one observes a pre-peak. The surprising thing is, however, that while this peak grows with increasing  $x$ , at the same time the upper band rapidly loses its intensity and weight is transferred to the low-energy region.<sup>1,2</sup> A similar effect has been observed in Li doped NiO.<sup>3</sup> This disappearance of weight from the upper band is totally unexpected from a single-particle point of view since the total intensity of a band is

always equal to the number of electrons it can accommodate, i.e., equals one per unit cell and per spin direction.

A similar rapid spectral-weight transfer has been observed in optical spectroscopy.<sup>4-6</sup> The strong interband transition observed in insulating  $\text{La}_2\text{CuO}_4$  around 2-3 eV rapidly loses weight, which reappears in the low-energy region ( $< 1$  eV) in the hole doped  $\text{La}_{1-x}\text{Sr}_x\text{CuO}_4$ . At the same time the total spectral intensity remains almost constant. This phenomenon has been observed in both electron and hole doped materials. This effect again cannot be explained by Bloch bands since then only a small decrease of the 2 eV feature is expected.

In this paper we will show that the observed intensity changes are exactly what is to be expected for correlated systems with  $U \gtrsim W_B$ , where  $W_B$  is the one-particle bandwidth. In order to understand the general physical principles behind the phenomena observed, we will simplify our discussion as much as possible and take the single-band Hubbard model as our starting point.

The well-known mapping of the Hubbard model onto the strong-coupling model in the large- $U$  limit leads to a decoupling of the various Hubbard bands and the band-index becomes a good quantum number. As a result, sum rules can be derived for the *individual* Hubbard bands. In 1967 Harris and Lange<sup>7</sup> considered this problem. They derived expressions for the intensities and energies of the two Hubbard bands for the one-particle spectrum to first order in  $t/U$ . In this article we will closely follow Harris and Lange. Their approach is extended to second order and a modified first-order expression is obtained which has the advantage that it is electron-hole symmetric. Furthermore, similar kind of expressions will be obtained for the optical spectrum. We will show that all sum-rule expectation values can be explicitly evaluated in one dimension using the Bethe-ansatz solution. The results will be compared with numerical-diagonalization data from small clusters for intermediate- $U$  values. This gives an estimate of the qualitative and quantitative accuracy of the derived expressions in the intermediate- $U$  range. It is our aim to give a relatively complete overview of quantities that can be obtained from the mapping. Therefore we will sometimes include previous results by Harris and Lange and others.

In recent years various numerical studies on the one-band and three-band Hubbard models have shown that these models can explain the observed rapid weight changes with doping very well.<sup>2,8-13</sup> However, such computer experiments by themselves do not give much insight into the physical origin of the observed weight changes. Unger and Fulde<sup>14</sup> calculated the one-particle spectrum of the three-band model using a projection operator formalism and found a similar weight transfer (see also Ref. 15). Since this approach describes accurately the local dressing of particles, it suggests that the effect has a *local* origin. This is also evidenced by the numerical data which show only a small dependence on cluster size.<sup>11</sup>

Because of the charge-transfer nature<sup>16</sup> of the CuO-based high- $T_c$  superconductors, it seems more reasonable to use a three-band model as a starting point to describe the electronic structure. However, the added holes have a strong tendency to form local singlets<sup>17,18</sup> and the cor-

responding triplet excitation is roughly 3.5 eV (Ref. 18) higher in energy for realistic parameters. This observation leads to a reduced Hilbert space consisting of Cu spins and "holes" (Zhang-Rice singlets), suggesting that a  $t$ - $J$  or single-band Hubbard model contains the essential dynamics for the electrons close to the chemical potential. This equivalence of the three- and the one-band model is further suggested by the similar low-energy spectrum observed in numerical calculations.<sup>19,20</sup> However, because of the doubtful validity of the usual perturbation approach in  $t_{pd}$ , the Cu-O hopping matrix element, this reduction from three bands to one band has remained an open issue. Recently various authors have proposed an alternative "cell" perturbation approach,<sup>21-25</sup> in which the  $\text{CuO}_2$  planes are divided into  $\text{CuO}_4$  cells. Then it can be shown that the intercell matrix elements are small compared to the intracell excitation energies and a quantitative derivation of an effective one-band model becomes possible.

In previous work<sup>8,11</sup> we have shown that the charge-transfer model in the ionic limit (small  $t_{pd}$ ) is asymmetric between hole and electron doping. On the one hand electrons behave like strongly correlated objects and the one-particle spectral weight is strongly doping dependent. On the other hand, oxygen holes behave like free particles. This asymmetry is removed for large values of  $t_{pd}$  and both electrons and holes show a correlated behavior. This can be explained in a natural way by splitting the contribution to the one-particle spectrum into an intercell and an intracell part.<sup>26</sup>

In order to make a quantitative comparison with experiment, matrix-element effects have to be taken into account. This is especially important for the O 1s spectra where the 1s electron is excited to a local O 2p level. Since the oxygen is in between two copper sites and therefore belongs to two  $\text{CuO}_2$  unit cells at the same time, this implies that the final states that can be reached have to obey the phase relation enforced by the 2p symmetry of the oxygen orbitals. Apart from this effect the 1s core hole in the final state also will influence the spectrum. In a multiband model with explicit oxygen degrees of freedom such effects are automatically taken into account.<sup>8,10-12</sup> Hybertsen *et al.*<sup>9</sup> have shown in detail how these matrix-element effects can be explicitly incorporated in a single-band Hubbard model approach. Also in the case of the optical spectra one would in principle expect different matrix elements for the lower and the upper bands since the microscopic current operator will make  $d$  to  $p$  transitions which in general will look different for Zhang-Rice singlets than for  $d^9$  spins. Here we do not intend to study the matrix-element effects associated with the three-band to one-band mapping,<sup>19-22</sup> but instead we shall focus on the correlation effects in the simplest and generic physical situation, where the relevant subspaces for the observed changes in the electronic structure are represented by the one-band Hubbard model.

The article is organized in the following way. First (in Sec. II) we will review how to construct the mapping from the Hubbard model to an effective Hamiltonian in which the band index is a good quantum number. We

will show how an arbitrary operator can be classified according to the number of doubly occupied sites it generates (annihilates) and introduce a transformation between the physical fermions and effective fermions which conserve the double occupancy. Using this formalism we obtain (in Sec. III) expressions for the  $\vec{k}$ -dependent occupation number, number of doubly occupied sites, and kinetic and potential energy. Next (in Sec. IV) we use the transformation of Sec. II to derive sum rules for the upper Hubbard band (UHB) and the lower (LHB) Hubbard band in the optical spectrum. In Sec. V similar sum rules are found for the one-particle spectrum up to second order in  $t/U$ . Apart from the total weight (zeroth moment) the average energy and width (first and second moment) also are discussed. In Sec. VI we compare the perturbation results with the closely related nonperturbative two-pole approach and discuss the  $\vec{k}$  dependence of the one-particle spectrum. The paper is concluded in Sec. VII.

## II. PERTURBATION THEORY: FORMALISM

The transformation of the Hubbard model<sup>27</sup> in the large- $U$  limit to the strong-coupling model or to the simpler  $t$ - $J$  model has a long history.<sup>7,28–33</sup> Anderson<sup>28</sup> showed (without explicitly writing down the Hamiltonian) that the model can be reduced to a nearest-neighbor spin Heisenberg model at half filling, with antiferromagnetic exchange coupling  $J = 4t^2/U$ , where  $t$  is the hopping and  $U$  is the on-site Coulomb repulsion. The strong-coupling model, which reduces to the  $t$ - $J$  model when the three-site hopping terms are neglected, was derived by Chao, Spalek, and Oleś in 1977.<sup>31</sup> Since then various authors derived effective Hamiltonians for the LHB away from half filling and up to eighth order. After the discovery of the high- $T_c$  superconductors many people rederived the first-order mapping, leading to the famous  $t$ - $J$  model, usually considered to be the minimal model which includes correlations in a realistic way.

The aim is to rewrite the Hubbard Hamiltonian in a block-diagonal form, in which each block is characterized by a conserved integer number of “effective” doubly occupied sites. [We will show later how one can express the (noninteger) physical double occupancy in terms of the transformed fermions.] In what follows we will closely follow the work of Harris and Lange<sup>7</sup> and MacDonald *et al.*<sup>33</sup> The Hubbard Hamiltonian reads

$$H = V + T = U \sum_i n_{i,\uparrow} n_{i,\downarrow} - t \sum_{i,\delta,\sigma} a_{i,\sigma}^\dagger a_{i+\delta,\sigma}. \quad (1)$$

Here the sums run over the  $N_a$  sites,  $i + \delta$  stands for the set of nearest neighbors of  $i$ , and  $t > 0$ .

In this paper two types of Fermi operators will be distinguished. The original bare fermions that occur in the Hubbard model are defined by  $a_{i\sigma}^\dagger$ , while  $c_{i\sigma}^\dagger$  represents the new dressed fermions that conserve double occupancy. For an arbitrary operator  $O$  we define an operator  $\tilde{O}$  by

$$O \equiv \mathbf{O}(a), \quad \tilde{O} \equiv \mathbf{O}(c), \quad (2)$$

i.e., the operator  $\tilde{O}$  is obtained from  $O$  by replacing the Fermi operators  $a_{i\sigma}$  by the transformed operators  $c_{i\sigma}$ . In particular,

$$\tilde{V} = U \sum_i \tilde{n}_{i\uparrow} \tilde{n}_{i\downarrow} \quad (3)$$

serves to identify to which Hubbard band a state belongs. Note that  $O$  and  $\tilde{O}$  are only equivalent in the  $U \rightarrow \infty$  limit.

We seek a unitary transformation

$$H = e^S \tilde{H} e^{-S} = \tilde{H} + [S, \tilde{H}] + \frac{1}{2}[S, [S, \tilde{H}]] + \dots \quad (4)$$

such that

$$[H, \tilde{V}] = 0. \quad (5)$$

Then the effective double occupation (in  $c_{i,\sigma}$  fermions) is a good quantum number and operators and vectors can be labeled accordingly,

$$O = \sum_{n \in \mathbb{Z}} O_{nU},$$

$$O_{nU} |mU, \alpha\rangle = \sum_{\beta} c_{\alpha\beta}(O) |(m+n)U, \beta\rangle, \quad (6)$$

where  $\alpha$  and  $\beta$  label the internal degrees of freedom of a particular Hubbard band  $mU$  and  $c_{\alpha\beta}(O)$  are coefficients depending on the expanded operator  $O$ . Therefore,

$$[O_{nU}, \tilde{V}] = -nU O_{nU}. \quad (7)$$

This will prove to be a very useful relation in the following.

With the above considerations the derivation of  $S$  is very short. First let us decompose  $\tilde{T}$  as

$$\tilde{T} = \tilde{T}_0 + \tilde{T}_U + \tilde{T}_{-U},$$

$$\tilde{T}_0 = -t \sum_{i,\delta,\sigma} [(1 - \tilde{n}_{i,\sigma}) c_{i,\sigma}^\dagger c_{i+\delta,\sigma} (1 - \tilde{n}_{i+\delta,\sigma})$$

$$+ \tilde{n}_{i,\sigma} c_{i,\sigma}^\dagger c_{i+\delta,\sigma} \tilde{n}_{i+\delta,\sigma}], \quad (8)$$

$$\tilde{T}_U = -t \sum_{i,\delta,\sigma} \tilde{n}_{i,\sigma} c_{i,\sigma}^\dagger c_{i+\delta,\sigma} (1 - \tilde{n}_{i+\delta,\sigma}),$$

$$\tilde{T}_{-U} = -t \sum_{i,\delta,\sigma} (1 - \tilde{n}_{i,\sigma}) c_{i,\sigma}^\dagger c_{i+\delta,\sigma} \tilde{n}_{i+\delta,\sigma}.$$

Equation (5) is fulfilled if  $S$  eliminates, order by order, all the terms  $H_{nU}$  with  $n \neq 0$  from the Hamiltonian. From Eq. (4) one finds, for the first-order  $S$ ,

$$[S^{(1)}, \tilde{V}] = -\tilde{T}_U - \tilde{T}_{-U}. \quad (9)$$

This equation is directly solved using Eq. (7),

$$S^{(1)} = \left( \tilde{T}_U - \tilde{T}_{-U} \right) \frac{1}{U} \quad (10)$$

and using the first-order  $S^{(1)}$  one finds

$$H = \tilde{V} + \tilde{T}_0 + \left[ \tilde{T}_U, \tilde{T}_{-U} \right] \frac{1}{U} + \left[ \tilde{T}_U - \tilde{T}_{-U}, \tilde{T}_0 \right] \frac{1}{U} + \dots \quad (11)$$

The second-order term in  $S$  has to remove the last term in the above equation. Using again identity (7) one finds straightforwardly

$$S^{(2)} = \left[ \tilde{T}_U + \tilde{T}_{-U}, \tilde{T}_0 \right] \frac{1}{U^2}. \quad (12)$$

This process can be continued to any desired order:<sup>33</sup>  $S^{(n)}$  generates  $H^{(n+1)}$  through Eq. (4) and the undesired part  $\sum_{m \neq 0} H_{mU}^{(n+1)}$  is then eliminated by  $S^{(n+1)}$ , which follows directly from Eq. (7). The  $n$ th-order Hamiltonian will contain terms connecting  $n$ th nearest neighbors.

The operators  $S$  and  $H$  can be written as sums over

products of  $\tilde{T}_{mU}$  operators<sup>33</sup> and one could therefore wonder whether the terms generated are all *local*, i.e., describing the dynamics of fermions within the nearest and next-nearest neighbors, if the expansion in Eq. (11) is terminated at second order (for instance, a single product of two or more  $\tilde{T}$  terms is certainly nonlocal). However, it is easily proven by induction that this is indeed the case. Suppose we have found  $S$  to order  $n$  and this is local. Then  $H$  is generated to order  $n+1$  using Eq. (4). Since this consists of a sum of nested commutators, this has to be local if  $S$  is local. The next-order  $S^{(n+1)}$  is proportional to the various terms in  $H^{(n+1)}$  and is therefore also a local operator.

Explicitly evaluating the commutator  $[\tilde{T}_U, \tilde{T}_{-U}]$ , one finds, for the Hubbard Hamiltonian up to second order,

$$\begin{aligned} H &= \tilde{V} + \tilde{T}_0 + \left[ \tilde{T}_U, \tilde{T}_{-U} \right] / U + \mathcal{O}(t^3/U^2) \\ &= \tilde{V} + H_{sc} + H_d + H_{de} + \mathcal{O}(t^3/U^2), \end{aligned} \quad (13)$$

where

$$\begin{aligned} H_{sc} &= -t \sum_{i,\delta,\sigma} (1 - \tilde{n}_{i,\sigma}) c_{i,\sigma}^\dagger c_{i+\delta,\sigma} (1 - \tilde{n}_{i+\delta,\sigma}) - t^2/U \sum_{i,\delta,\sigma} [(1 - \tilde{n}_{i,\sigma}) \tilde{n}_{i,\sigma} \tilde{n}_{i+\delta,\sigma} (1 - \tilde{n}_{i+\delta,\sigma}) - c_{i,\sigma}^\dagger c_{i+\delta,\sigma}^\dagger c_{i+\delta,\sigma} c_{i,\sigma}] \\ &\quad - t^2/U \sum_{i,\delta,\delta',\sigma;\delta \neq \delta'} [(1 - \tilde{n}_{i+\delta,\sigma}) c_{i+\delta,\sigma}^\dagger \tilde{n}_{i,\sigma} (1 - \tilde{n}_{i,\sigma}) c_{i+\delta',\sigma} (1 - \tilde{n}_{i+\delta',\sigma}) \\ &\quad - (1 - \tilde{n}_{i+\delta,\sigma}) c_{i+\delta,\sigma}^\dagger c_{i,\sigma}^\dagger c_{i,\sigma} c_{i+\delta',\sigma} (1 - \tilde{n}_{i+\delta',\sigma})], \\ H_d &= -t \sum_{i,\delta,\sigma} \tilde{n}_{i,\sigma} c_{i,\sigma}^\dagger c_{i+\delta,\sigma} \tilde{n}_{i+\delta,\sigma} + t^2/U \sum_{i,\delta,\delta',\sigma;\delta \neq \delta'} [\tilde{n}_{i+\delta,\sigma} c_{i+\delta,\sigma}^\dagger \tilde{n}_{i,\sigma} (1 - \tilde{n}_{i,\sigma}) c_{i+\delta',\sigma} \tilde{n}_{i+\delta',\sigma} \\ &\quad + \tilde{n}_{i+\delta,\sigma} c_{i+\delta,\sigma}^\dagger c_{i,\sigma}^\dagger c_{i,\sigma} c_{i+\delta',\sigma} \tilde{n}_{i+\delta',\sigma}], \\ H_{de} &= +2t^2/U \sum_{i,\delta} (1 - \tilde{n}_{i,\uparrow})(1 - \tilde{n}_{i,\downarrow}) \tilde{n}_{i+\delta,\uparrow} \tilde{n}_{i+\delta,\downarrow} + 2t^2/U \sum_{i,\delta} c_{i,\uparrow}^\dagger c_{i,\downarrow}^\dagger c_{i+\delta,\downarrow} c_{i+\delta,\uparrow} \\ &\quad + t^2/U \sum_{i,\delta,\delta',\sigma;\delta \neq \delta'} [c_{i,\sigma}^\dagger c_{i,\sigma}^\dagger c_{i+\delta',\sigma} c_{i+\delta,\sigma} \tilde{n}_{i+\delta,\sigma} (1 - \tilde{n}_{i+\delta',\sigma}) + \text{H.c.}] \\ &\quad - t^2/U \sum_{i,\delta,\delta',\sigma;\delta \neq \delta'} [(1 - \tilde{n}_{i+\delta,\sigma}) c_{i+\delta,\sigma}^\dagger \tilde{n}_{i,\sigma} \tilde{n}_{i,\sigma} c_{i+\delta',\sigma} (1 - \tilde{n}_{i+\delta',\sigma}) \\ &\quad - \tilde{n}_{i+\delta,\sigma} c_{i+\delta,\sigma}^\dagger (1 - \tilde{n}_{i,\sigma}) (1 - \tilde{n}_{i,\sigma}) c_{i+\delta',\sigma} \tilde{n}_{i+\delta',\sigma}]. \end{aligned} \quad (14)$$

The Hamiltonian contains three terms. The strong-coupling part (or  $t$ - $J$  model including three-site hopping)  $H_{sc}$  describes the motion of holes in the spin background.  $H_d$  does the same for doubly occupied sites and can, apart from the second term, be obtained from  $H_{sc}$  by an electron-hole transformation and a sign change of  $t$ .  $H_{de}$  acts only if there are doubly occupied and empty sites on neighboring places, i.e., describes excitations with en-

ergy  $nU$ ,  $n > 0$ . For less than half filling the states in the LHB are fully described by  $H_{sc}$  only. We note that the terms  $\sim t^2/U$  stand for the superexchange interaction (the  $J$ -term of the  $t$ - $J$  model with  $J = 4t^2/U$ ) and the three-site hopping term. Thus the strong-coupling model  $H_{sc}$  for the LHB is *not* equivalent to the  $t$ - $J$  model. The three-site hopping part is often neglected using the argument that, for a small doping percentage  $x$ , it adds only

an amount  $\sim xJ$  to the total energy per site. We shall discuss the significance and physical consequences of the three-site hopping term in the following sections.

In this paper we study the effect of the transformation  $S$  on operators  $O$ ,

$$O = e^S \tilde{O} e^{-S} = \tilde{O} + [S, \tilde{O}] + \frac{1}{2}[S, [S, \tilde{O}]] + \dots \quad (15)$$

Using the second-order expression for  $S$  the above formula is expanded to

$$\begin{aligned} O_{nU} = \tilde{O}_{nU} + \frac{1}{U} [\tilde{T}_U, \tilde{O}_{(n-1)U}] - \frac{1}{U} [\tilde{T}_{-U}, \tilde{O}_{(n+1)U}] + \frac{1}{U^2} ([[\tilde{T}_U, \tilde{T}_0], \tilde{O}_{(n-1)U}] + [[\tilde{T}_{-U}, \tilde{T}_0], \tilde{O}_{(n+1)U}] \\ + \frac{1}{2}[\tilde{T}_U, [\tilde{T}_U, \tilde{O}_{(n-2)U}]] - \frac{1}{2}[\tilde{T}_U, [\tilde{T}_{-U}, \tilde{O}_{nU}]] - \frac{1}{2}[\tilde{T}_{-U}, [\tilde{T}_U, \tilde{O}_{nU}]] + \frac{1}{2}[\tilde{T}_{-U}, [\tilde{T}_{-U}, \tilde{O}_{(n+2)U}]]). \end{aligned} \quad (17)$$

In the following sections we will exploit this formula to derive partial sum rules for the individual Hubbard bands for the one-particle and optical spectra.

Of special interest is the decomposition of the fermion operators themselves,

$$\begin{aligned} c_{i,\sigma} &= c_{i,\sigma;0} + c_{i,\sigma;-U}, \\ c_{i,\sigma;0} &= c_{i,\sigma}(1 - \tilde{n}_{i,\bar{\sigma}}), \\ c_{i,\sigma;-U} &= c_{i,\sigma} \tilde{n}_{i,\bar{\sigma}}. \end{aligned} \quad (18)$$

The occupation-number operator conserves double occupancy and therefore  $\tilde{n}_{i,\sigma} = \tilde{n}_{i,\sigma;0}$ . Explicit evaluation of Eq. (15) to first order gives

$$\begin{aligned} a_{i,\sigma} &= c_{i,\sigma} - \frac{t}{U} \sum_{\delta} \{(\tilde{n}_{i+\delta,\bar{\sigma}} - \tilde{n}_{i,\bar{\sigma}}) c_{i+\delta,\sigma} \\ &\quad - c_{i+\delta,\bar{\sigma}}^{\dagger} c_{i,\sigma} c_{i,\bar{\sigma}} + c_{i,\bar{\sigma}}^{\dagger} c_{i,\sigma} c_{i+\delta,\bar{\sigma}}\}. \end{aligned} \quad (19)$$

We stress that  $c_{i,\sigma}$  and  $a_{i,\sigma}$  are not related through  $c_{i,\sigma} = a_{i,\sigma}(1 - n_{i,\bar{\sigma}})$ .

### III. EXPECTATION VALUES

Before focusing on spectral properties we will show how expectation values of operators in the Hubbard model can be expressed in terms of the rotated operators  $c_{i,\sigma}$ . This will be especially helpful in those cases where the lowest-order operator in the strong-coupling case has a simple form. Expressions will be obtained for the double occupancy and the  $\vec{k}$ -dependent occupation number  $n_{\vec{k}}$ .

Although the strong-coupling model does not contain explicitly doubly occupied sites, there still exists a direct relation between the potential energy in the Hubbard model and observables in the strong-coupling formulation. The potential energy to second order in  $t$  is [see Eq. (16)]

$$\begin{aligned} V = \tilde{V} + \frac{1}{U} [\tilde{T}_U - \tilde{T}_{-U}, \tilde{V}] + \frac{1}{U^2} ([[\tilde{T}_U + \tilde{T}_{-U}, \tilde{T}_0], \tilde{V}] \\ + \frac{1}{2} [\tilde{T}_U - \tilde{T}_{-U}, [\tilde{T}_U - \tilde{T}_{-U}, \tilde{V}]]). \end{aligned} \quad (20)$$

Since the ground state contains no double occupancy in  $c_{i,\sigma}$  for less than half filling the expressions for ground-state expectation values  $\langle \rangle$  simplify considerably using

$$\begin{aligned} O = \tilde{O} + \frac{1}{U} [\tilde{T}_U - \tilde{T}_{-U}, \tilde{O}] \\ + \frac{1}{U^2} ([[\tilde{T}_U + \tilde{T}_{-U}, \tilde{T}_0], \tilde{O}] \\ + \frac{1}{2} [\tilde{T}_U - \tilde{T}_{-U}, [\tilde{T}_U - \tilde{T}_{-U}, \tilde{O}]]). \end{aligned} \quad (16)$$

The wonderful outcome of the above exercise is that, because the rotated operators  $\tilde{O}$  can be directly decomposed into parts creating a particular number of doubly occupied sites  $n$  [Eq. (2)], one can obtain such an expansion for the *original* operators as well. Using Eq. (16) one finds, to second order,

$$\langle \tilde{O}_{nU} \rangle = 0 \quad \text{when } n \neq 0. \quad (21)$$

In the case of finite temperatures the ground-state expectation value has to be replaced by the thermal average. The above equation will, however, still be a good approximation when the temperature  $T \ll U$ .

Using Eq. (7) it is easy to show that the expectation value of the potential energy becomes  $\langle \tilde{V} \rangle = 0$

$$\langle V \rangle = -\frac{1}{U} \langle [\tilde{T}_U, \tilde{T}_{-U}] \rangle. \quad (22)$$

For the kinetic energy one finds, to the same order in  $t/U$ ,

$$\begin{aligned} T = \tilde{T}_{-U} + \tilde{T}_0 + \tilde{T}_U + \frac{1}{U} [\tilde{T}_U - \tilde{T}_{-U}, \tilde{T}_{-U} + \tilde{T}_0 + \tilde{T}_U], \\ \langle T \rangle = \langle \tilde{T}_0 \rangle + \frac{2}{U} \langle [\tilde{T}_U, \tilde{T}_{-U}] \rangle. \end{aligned} \quad (23)$$

Combining Eqs. (22) and (24) one finds a kind of virial relationship between the second-order corrections to the kinetic and the potential energy

$$\langle T^{(2)} \rangle = -2 \langle V^{(2)} \rangle \quad (24)$$

and  $T^{(2)} + V^{(2)} = H^{(2)}$ , where  $H^{(2)}$  is the second-order term in the strong-coupling Hamiltonian given by Eq. (14). This is a general feature of perturbation theory. The (kinetic) energy gain due to the perturbation is twice the energy loss in the unperturbed part.

To be more explicit one finds, for the double occupation on site  $i$ ,

$$\begin{aligned} \langle n_{i,\uparrow} n_{i,\downarrow} \rangle = -\frac{2t^2}{U^2} \sum_{\delta} \langle \tilde{S}_i \cdot \tilde{S}_{i+\delta} - \frac{1}{4} \tilde{n}_i \tilde{n}_{i+\delta} \rangle \\ + \frac{t^2}{U^2} \sum_{\delta, \delta', \sigma; \delta \neq \delta'} \langle c_{i+\delta, \sigma}^{\dagger} \tilde{n}_{i, \bar{\sigma}} c_{i+\delta', \sigma} \\ - c_{i+\delta, \sigma}^{\dagger} c_{i, \bar{\sigma}} c_{i, \sigma} c_{i+\delta', \bar{\sigma}} \rangle. \end{aligned} \quad (25)$$

Here we have split the sum into a two- and three-site part and  $n_i \equiv \sum_{\sigma} n_{i,\sigma}$ . At half filling the three-site term does not contribute and the amount of double occupation is entirely determined by the spin order. This expresses the

fact that spin exchange is caused by virtual states with the two spins on the same site. If the spin would be able to form a complete singlet with all its neighbors, the term in the expectation value would be equal to  $-1$  and the amount of double occupancy would be  $2zt^2/U^2$ , where  $z$  is the number of nearest neighbors. For a ferromagnetic alignment of the spins the double occupation is zero.

So far, all the derived relations were general. Since the explicit evaluation of the above formulas is possible in one dimension, we present particular results for a one-dimensional (1D) Hubbard model. In one dimension the ground-state energy per site for large  $U$  is<sup>34</sup>

$$E_0 = -2t \frac{\sin(n\pi)}{\pi} - 4 \ln 2 \frac{t^2}{U} n^2 \left( 1 - \frac{\sin(2n\pi)}{2n\pi} \right), \quad (26)$$

where  $n$  is the particle density. Using Eq. (24) one finds

$$\langle n_{i,\uparrow} n_{i,\downarrow} \rangle = 4 \ln 2 \frac{t^2}{U^2} n^2 \left( 1 - \frac{\sin(2n\pi)}{2n\pi} \right) + \mathcal{O}(t^3/U^3). \quad (27)$$

In fact, there are two alternative ways to obtain the same result. First, the number of doubly occupied sites is equal to the derivative of the energy with respect to  $U$ . Second, one can explicitly evaluate Eq. (25) using the Ogata-Shiba wave function.<sup>35</sup> We will come back to this in Sec. IV.

In Fig. 1 the amount of double occupation given by Eq. (27) is plotted as a function of the particle density  $n$ . The large- $U$  expansion is compared with Lanczos diagonalization data for a ten-site ring, for three different values of  $U$ . For intermediate- $U$  values the second-order expression clearly overestimates the amount of double occupancy. However, the curves are qualitatively similar to the numerical data. Deviations are of the order of 40% for  $U = 5$ . For very large  $U$  level crossings occur for particle numbers with open-shell configurations, and the ground states with different values of total momenta are stabilized in place of those which follow from the one-particle picture. In these cases the amount of double occupancy is suppressed. The numerical values for  $n = 0.2$ ,  $n = 0.6$ , and  $n = 1$  (closed shell) agree well with the second-order expression at  $U = 100$ .

Another interesting quantity is the  $\vec{k}$ -dependent occupation number

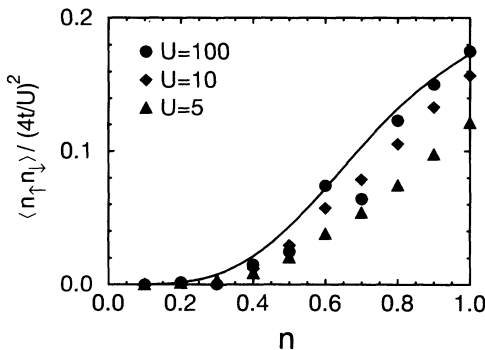


FIG. 1. The number of doubly occupied sites, in units of  $(4t/U)^2$ , as a function of electronic filling  $n$ . The line is the second-order result Eq. (27) and the points are from the numerical ground state of a ten-site ring for  $U = 100, 10$ , and  $5$  ( $t = 1$ ).

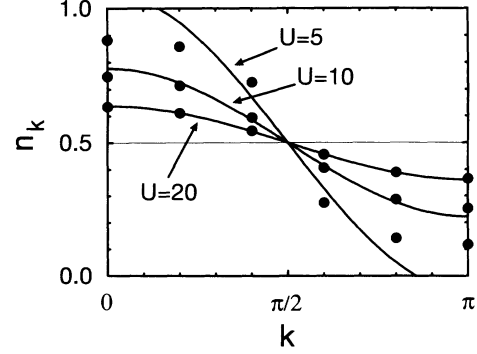


FIG. 2. The  $k$ -dependent occupation number  $n_{\vec{k}}$  for the 1D Hubbard model at half filling for  $U = 20, 10$ , and  $5$  ( $t = 1$ ). The lines and the points correspond to first order in the  $t/U$  result Eq. (31) and to  $n_{\vec{k}}$  obtained from the numerical ground state of a ten-site ring.

$$n_{\vec{k},\sigma} = \frac{1}{N_a} \sum_{i,j} e^{i\vec{k}\cdot(\vec{R}_i - \vec{R}_j)} \langle a_{i,\sigma}^\dagger a_{j,\sigma} \rangle. \quad (28)$$

Using Eq. (19) and the fact that the ground state has zero double occupation in  $c_{i,\sigma}$  fermions, one finds

$$n_{\vec{k},\sigma} = \tilde{n}_{\vec{k},\sigma} + \frac{t}{N_a U} \sum_{i,\delta,j} \cos[\vec{k}\cdot(\vec{R}_i - \vec{R}_j)] \times \langle c_{i+\delta,\sigma}^\dagger \tilde{n}_{i,\bar{\sigma}} c_{j,\sigma} - c_{i+\delta,\bar{\sigma}}^\dagger c_{i,\sigma} c_{i,\bar{\sigma}} c_{j,\sigma} \rangle. \quad (29)$$

In the Hubbard model with nearest-neighbor hopping (1) one defines the one-particle energies as

$$\epsilon_{\vec{k}} = -t \sum_{\delta} e^{i\vec{k}\cdot(\vec{R}_i - \vec{R}_{i+\delta})}. \quad (30)$$

At half filling Eq. (29) becomes therefore particularly simple (see also Ref. 32),

$$n_{\vec{k}} = \frac{1}{2} + 2 \frac{\epsilon_{\vec{k}}}{U} \left\langle \tilde{S}_i \cdot \tilde{S}_{i+\delta} - \frac{1}{4} \right\rangle. \quad (31)$$

Therefore, the entire  $\vec{k}$  dependence is determined by the one-particle dispersion  $\epsilon_{\vec{k}}$ .

In Fig. 2 we compare the above result at half filling with a numerical calculation of  $n_{\vec{k}}$  for a ten-site ring. The Bethe-ansatz result for the spin-spin correlation function  $\langle \tilde{S}_i \cdot \tilde{S}_{i+\delta} \rangle - 1/4 = -\ln 2$  is used. From the figure one can see that the correction to the value  $1/2$  is not small, even for  $U/t$  as large as 20. However, already the first-order term gives a good description of the  $t$  dependence in the strong- and intermediate-coupling regime. In general operators have sizable first-order corrections when written in terms of strong-coupling Fermi operators. This should be kept in mind when comparing results for the Hubbard model with those of the strong-coupling or  $t$ - $J$  model.

#### IV. OPTICAL SPECTROSCOPY

In this section we will use the above formalism to derive expressions for the total optical sum rule and partial sum rules for the two Hubbard bands. First the current and sum-rule expressions for the Hubbard model will be transformed to their strong-coupling form by replacing the  $a_{i,\sigma}$  operators by the corresponding expression in terms of  $c_{i,\sigma}$  operators. Then the operators are split into an inter- and an intraband part and these decomposed

operators will be used to calculate the sum rules for the LHB and the UHB.

The usual way to treat optical spectroscopy<sup>36</sup> is to assume the electric field in the  $x$  direction and to start from the  $x$  component of the polarization operator  $P_x = \sum_{i,\sigma} R_{i,x} n_{i,\sigma}$ , with  $R_{i,x}$  standing for the  $x$  component of the position vector of atom  $i$ . The ‘‘paramagnetic’’ particle current is the time derivative of the polarization

$$j_x = i[H, P_x] = it \sum_{i,\delta,\sigma} \delta_x a_{i+\delta,\sigma}^\dagger a_{i,\sigma}. \quad (32)$$

As before  $\vec{\delta}$  is a vector connecting nearest-neighbor sites. In the following we will discuss a (finite) system with open boundary conditions, where no zero-frequency Drude peak occurs. However, the final sum-rule expressions [see Eqs. (38), (39), and (41)] are valid for periodic boundary conditions as well.<sup>37</sup>

Using linear-response theory one finds, for the real part of the conductivity per site,<sup>36,38–40</sup>

$$\sigma_x(\omega) = \frac{1}{\omega N_a} \sum_f |\langle f, N | j_x | 0, N \rangle|^2 \delta(\omega - E_f + E_0). \quad (33)$$

Replacing one of the current operators with  $i[H, P_x]$ , one obtains an extra term  $E_f - E_0 = \omega$  in the above equation, canceling the  $\omega^{-1}$  factor in Eq. (33). Now the integral over  $\omega$  absorbs the  $\delta$  function and the sum over final states  $f$  is the identity operator. Therefore the total sum rule  $W$  is

$$W \equiv \int_0^\infty \sigma_x d\omega = \frac{i}{2N_a} \langle [j_x, P_x] \rangle = -\frac{1}{2N_a} \langle T_x \rangle, \quad (34)$$

where the last relation in Eq. (34) holds only for the nearest-neighbor hopping model, and the distance between nearest neighbors is set equal to 1. The sum rule (34) expressed in terms of the commutator of the current and polarization will be our starting point in the following.

To obtain expressions for the sum rules of the individual Hubbard bands the current and polarization operator have to be decomposed as in Eq. (6). Using Eq. (19) the polarization operator to first order becomes

$$\begin{aligned} P_x &= P_{x,-U} + P_{x,0} + P_{x,U} + \mathcal{O}(t^2/U^2), \\ P_{x,U} &= -\frac{t}{U} \sum_{i,\sigma} \left[ \tilde{n}_{i,\sigma} c_{i+\hat{x},\sigma}^\dagger c_{i,\sigma} (1 - \tilde{n}_{i+\hat{x},\sigma}) \right. \\ &\quad \left. - \tilde{n}_{i+\hat{x},\sigma} c_{i+\hat{x},\sigma}^\dagger c_{i,\sigma} (1 - \tilde{n}_{i,\sigma}) \right], \end{aligned} \quad (35)$$

$$\begin{aligned} P_{x,0} &= \sum_{i,\sigma} R_{i,x} \tilde{n}_{i,\sigma}, \\ P_{x,-U} &= -\frac{t}{U} \sum_{i,\sigma} \left[ (1 - \tilde{n}_{i+\hat{x},\sigma}) c_{i+\hat{x},\sigma}^\dagger c_{i,\sigma} \tilde{n}_{i,\sigma} \right. \\ &\quad \left. - (1 - \tilde{n}_{i,\sigma}) c_{i,\sigma}^\dagger c_{i+\hat{x},\sigma} \tilde{n}_{i+\hat{x},\sigma} \right]. \end{aligned}$$

Since  $\tilde{n}_{i,\sigma} = \tilde{n}_{i,\sigma,0}$  the polarization operator does not cause transitions to the UHB to lowest order and the weight of the UHB is of order  $t^2/U$ . The current operator to second order is

$$\begin{aligned} j_x &= it \sum_{i,\delta,\sigma} \delta_x c_{i+\delta,\sigma}^\dagger c_{i,\sigma} + i \frac{t^2}{U} \sum_{i,\delta,\delta',\sigma} (\delta_x - \delta'_x) \\ &\quad \times \left( c_{i+\delta,\sigma}^\dagger \tilde{n}_{i,\sigma} c_{i+\delta',\sigma} - c_{i+\delta,\sigma}^\dagger c_{i,\sigma} c_{i+\delta',\sigma} \right) \end{aligned} \quad (36)$$

and, for instance,

$$\begin{aligned} j_{x,U} &= it \sum_{i,\delta,\sigma} \delta_x \tilde{n}_{i+\delta,\sigma} c_{i+\delta,\sigma}^\dagger c_{i,\sigma} (1 - \tilde{n}_{i,\sigma}) \\ &\quad + i \frac{t^2}{U} \sum_{i,\delta,\delta',\sigma} (\delta_x - \delta'_x) [\tilde{n}_{i+\delta,\sigma} c_{i+\delta,\sigma}^\dagger \tilde{n}_{i,\sigma} c_{i+\delta',\sigma} \\ &\quad \times (1 - \tilde{n}_{i+\delta',\sigma}) - \tilde{n}_{i+\delta,\sigma} c_{i+\delta,\sigma}^\dagger c_{i,\sigma} c_{i+\delta',\sigma} \\ &\quad \times (1 - \tilde{n}_{i+\delta',\sigma})]. \end{aligned} \quad (37)$$

The current does cause excitations to the UHB in lowest order.

The total sum rule is proportional to the kinetic energy in the  $x$  direction. For cubic lattices this is just the total kinetic energy divided by the dimension. Using the previous result Eq. (24) (see also Ref. 41),

$$\begin{aligned} W &= -\frac{1}{zN_a} \langle \tilde{T} \rangle + \frac{2t^2}{zUN_a} \sum_{i,\delta,\delta',\sigma} \left\langle c_{i+\delta,\sigma}^\dagger \tilde{n}_{i,\sigma} c_{i+\delta',\sigma} \right. \\ &\quad \left. - c_{i+\delta,\sigma}^\dagger c_{i,\sigma} c_{i+\delta',\sigma} \right\rangle + \mathcal{O}(t^3/U^2), \end{aligned} \quad (38)$$

with  $z$  being the number of nearest neighbors. If the distinction between the  $a_{i,\sigma}$  and the  $c_{i,\sigma}$  Fermi operators is not made, only the first-order term proportional to the expectation value of  $\tilde{T}$  is obtained. The expectation values refer to the ground state of the strong-coupling model.

Using Eq. (35) and (36) we obtain, for the weight of the LHB,

$$\begin{aligned} W_0 &= \frac{i}{2N_a} \langle [j_{x,0}, P_{x,0}] \rangle \\ &= -\frac{1}{zN_a} \langle \tilde{T} \rangle \\ &\quad + \frac{t^2}{2UN_a} \sum_{i,\delta,\delta',\sigma} (\delta_x - \delta'_x)^2 \left\langle c_{i+\delta,\sigma}^\dagger \tilde{n}_{i,\sigma} c_{i+\delta',\sigma} \right. \\ &\quad \left. - c_{i+\delta,\sigma}^\dagger c_{i,\sigma} c_{i+\delta',\sigma} \right\rangle + \mathcal{O}(t^3/U^2). \end{aligned} \quad (39)$$

Note that in between the current and polarization operator there is still the complete set of final states  $|f, N\rangle$  [compare with Eq. (33)]. Because both  $j_{x,0}$  and  $P_{x,0}$  do not create doubly occupied sites in  $c_{i,\sigma}$ , only final states in the LHB are reached and therefore  $W_0$  is the sum rule for the LHB. From the above equation it is clear that  $W_0$  vanishes at half filling. The weight in the UHB is

$$\begin{aligned} W_U &= \frac{i}{2N_a} \langle j_{x,-U} P_{x,U} - P_{x,-U} j_{x,U} \rangle \\ &= \frac{t^2}{UN_a} \sum_{i,\delta,\delta',\sigma} \delta_x \delta'_x \left\langle c_{i+\delta,\sigma}^\dagger \tilde{n}_{i,\sigma} c_{i+\delta',\sigma} \right. \\ &\quad \left. - c_{i+\delta,\sigma}^\dagger c_{i,\sigma} c_{i+\delta',\sigma} \right\rangle + \mathcal{O}(t^3/U^2), \end{aligned} \quad (40)$$

which is conveniently rewritten to

$$\begin{aligned} W_U &= -\frac{4t^2}{UN_a} \sum_i \left\langle \tilde{S}_i \cdot \tilde{S}_{i+\hat{x}} - \frac{1}{4} \tilde{n}_i \tilde{n}_{i+\hat{x}} \right\rangle \\ &\quad - \frac{2t^2}{UN_a} \sum_{i,\sigma} \left\langle c_{i-\hat{x},\sigma}^\dagger \tilde{n}_{i,\sigma} c_{i+\hat{x},\sigma} \right. \\ &\quad \left. - c_{i-\hat{x},\sigma}^\dagger c_{i,\sigma} c_{i+\hat{x},\sigma} \right\rangle + \mathcal{O}(t^3/U^2). \end{aligned} \quad (41)$$

Equations (39) and (41) show that the UHB and the LHB measure different parts of the three-site hopping. In a 2D system the  $t^2/U$  term consists of three distinct processes: (i) “backward hopping” equivalent to the  $\vec{S}_i \cdot \vec{S}_{i+\delta}$  term, (ii) “forward hopping” in the  $x$  ( $y$ ) direction to third neighbors at a distance 2, and (iii) “sideward hopping” to neighbors at a distance  $\sqrt{2}$ . The total sum rule  $W$  (38) consists of the first-order term  $\sim -\langle T \rangle/z$ , while the second-order term involves the sum of these three independent contributions. At half filling the UHB, however, gets all its intensity from the backward hopping and for finite doping the weight is *reduced* by the forward-hopping term. We note that the latter hopping term is neglected in the frequently studied  $t$ - $J$  model and thus the optical spectra of the strong-coupling model and the  $t$ - $J$  model are quite different. The weight of the LHB (39) is largely determined by the forward term. The prefactor is  $(\delta_x - \delta'_x)^2 = 4$  and half of this consists of transferred weight from the UHB. [Note that the sum of (39) and (40) gives the total  $W$  (38).] Only the LHB weight contains contributions from the sideward hopping term. Since the backward hopping does not contribute to the LHB, the weight of the LHB vanishes at half filling.

In one dimension all expectation values can be found using the Bethe-ansatz results. Ogata and Shiba<sup>35</sup> showed that for large  $U$  the Bethe-ansatz equations decouple and the spin and charge of the electrons completely separate. The wave function is a product of a spinless-fermion single-Slater-determinant wave function for the charge and a spin wave function which is the solution of a “squeezed” Heisenberg spin chain with  $N$  (not  $N_a$ ) sites, where  $N \leq N_a$  is the number of electrons. Although this is a major simplification, the actual calculation of large-distance expectation values, such as  $\langle n_k \rangle$ , is still involved.<sup>35</sup> Since the wave function does not contain doubly occupied sites it is equal to the wave function of the Hubbard model only to zeroth order. However, Ogata and Shiba demonstrated that the energy expectation value of the wave function using the strong-coupling model gives the correct ground-state energy of the Hubbard model to order  $t^2/U$ . Therefore, the spin and charge correspond to the  $c_{i,\sigma}$  fermions and not the  $a_{i,\sigma}$  fermions and for the strong-coupling model the wave function is correct to first order.

For the sum rules derived above only up to next-nearest-neighbor expectation values have to be calculated. As an example we will show explicitly how to calculate the forward-hopping process in Eq. (41),<sup>35</sup>

$$\sum_{\sigma} \langle c_{i-1,\sigma}^{\dagger} \tilde{n}_{i,\bar{\sigma}} c_{i+1,\sigma} - c_{i-1,\sigma}^{\dagger} c_{i,\bar{\sigma}}^{\dagger} c_{i,\sigma} c_{i+1,\bar{\sigma}} \rangle. \quad (42)$$

The charge dynamics is the same in both terms, i.e., the spinless fermion hops from site  $i+1$  to site  $i-1$  if site  $i$  is occupied. The expectation value of the hopping for a Slater determinant of  $k$  states filled up to the spinless-fermion (SF) Fermi wave vector  $k_F^{\text{SF}} = 2k_F = \pi N/N_a = \pi n$  is

$$\langle c_{i-1}^{\dagger} \tilde{n}_i c_{i+1} \rangle_{\text{SF}} = n \frac{\sin(2\pi n)}{2\pi} - \frac{\sin^2(\pi n)}{\pi^2}. \quad (43)$$

The spin part involves only two nearest-neighbor sites in a Heisenberg chain (the holes are squeezed out). The first

term flips two antiparallel neighboring spins and is equal to  $S_i^+ S_{i+1}^- + S_i^- S_{i+1}^+$ . The second term checks whether the two spins are antiparallel and is  $2S_i^z S_{i+1}^z - 1/2$ . The spin part of the expectation value is therefore

$$2\langle \vec{S}_i \cdot \vec{S}_{i+1} - \frac{1}{4} \rangle_{\text{Heisenberg}} = -2 \ln 2. \quad (44)$$

The total expectation value Eq. (42) is the product of the spin and the charge expectation values above.

The other expectation values can be calculated in a similar way and the sum rules in one dimension to order  $t^2/U$  are found to be

$$W = t \frac{\sin(\pi n)}{\pi} + 4 \ln 2 \frac{t^2}{U} \left( n^2 - n \frac{\sin(2\pi n)}{2\pi} \right), \quad (45)$$

$$W_0 = t \frac{\sin(\pi n)}{\pi} - 8 \ln 2 \frac{t^2}{U} \left( n \frac{\sin(2\pi n)}{2\pi} - \frac{\sin^2(\pi n)}{\pi^2} \right), \quad (46)$$

$$W_U = 4 \ln 2 \frac{t^2}{U} \left( n^2 + n \frac{\sin(2\pi n)}{2\pi} - 2 \frac{\sin^2(\pi n)}{\pi^2} \right). \quad (47)$$

Baeriswyl *et al.*<sup>42</sup> calculated the total oscillator strength at half filling. Their result is consistent with the above expression for  $W$ .

The zero-frequency Drude weight  $D$  in one dimension can be expressed in terms of the charge velocity  $u_{\rho}$  and the compressibility  $K_{\rho}$  (see Ref. 43). Writing  $\sigma(\omega) = D\delta(\omega) + (\text{finite frequency part})$ ,

$$D = 2K_{\rho} u_{\rho} = \pi u_{\rho}^2 \left( \frac{d^2 E_0(n)}{dn^2} \right)^{-1}, \quad (48)$$

where  $E_0$  is the ground-state energy per site in the Hubbard model as given in Eq. (26). The charge velocity,<sup>44</sup> to second order,

$$u_{\rho} = 2t \sin(\pi n) - \frac{8t^2}{U} \ln 2n \sin(2\pi n). \quad (49)$$

Comparing with Eq. (46) we find that to order  $t^2/U$ ,  $W_0$  and  $D$  are the same,

$$W_0 = D + \mathcal{O}(t^3/U^2). \quad (50)$$

The conductivity in one dimension can therefore be divided into three parts: a Drude weight of order  $t$ , an UHB of order  $t^2/U$ , and a finite-frequency (incoherent) intensity in the LHB of order  $t^3/U^2$ . This agrees with the recent result of Horsch and Stephan,<sup>45</sup> who showed that for one hole the finite-frequency signal in the  $t$ - $J$  and the strong-coupling model are proportional to  $J^2/t$ , due to spin-charge interaction. This behavior should be contrasted with that observed in two dimensions, where the finite-frequency weight in the LHB is proportional to  $t$ . However, we stress that the weight transfer from UHB to LHB is qualitatively independent of dimension, as will be shown later. Only the weight distribution *inside* the LHB itself is very sensitive on spin-charge separation. If the separation is complete, as in the Ogata-Shiba wave function, the current acts on the spinless fermion part only

and all the weight goes into the Drude peak. If charge and spin do not decouple the electrons will scatter to finite-frequency states. This argument, however, applies only to the LHB since the current causes excitations to the UHB in any dimension, independent of spin-charge decoupling.

The optical experiments on the cuprate materials show a fast decrease in intensity of the 2-eV feature with increasing doping  $x$ .<sup>4,5</sup> However, if one interprets the low-energy and 2-eV features in the experiments as a single-particle valence and conduction band, the intensity of the UHB should remain almost constant. This weight is roughly proportional to the number of  $\vec{k}$ -conserving interband transitions. For a doping of  $x = 1 - n$  holes per unit cell of a Mott-Hubbard insulator one expects therefore  $W_{\text{interband}}(x) = (1-x)W_{\text{interband}}(x=0)$  [while for an ordinary insulator the prefactor would be  $(1-x/2)$ ]. For a typical doping  $x = 0.2$  this would imply an intensity reduction of the 2-eV feature by only 20%.

In Eq. (41) the weight of the UHB is determined by the spin-spin expectation value. At half filling this term is proportional to the number of neighbor bonds times the nearest-neighbor spin correlation function. If one hole is introduced, this will remove two bonds from the sum [see Fig. 3(a)] and therefore  $W_U = (1-2x)W_U(x=0)$ . The UHB loses its weight twice as fast as expected for the Mott-Hubbard insulator and four times faster than in a semiconductor. In more than one dimension the reduction of the UHB weight can be expected to go even faster since the spin correlations weaken with increasing  $x$ . The fast transfer of weight in the optical spectrum is related to the dilution of the spin system and the decrease of antiferromagnetic spin correlations.

It is easy to understand why  $\langle \vec{S}_i \cdot \vec{S}_{i+\delta} \rangle$  appears in Eq. (41) [see Fig. 3b]. The current moves an electron from site  $i$  to site  $i + \delta$ . It will cause a transition to the UHB if first site  $i + \delta$  is occupied and second if the spin on site  $i$  is antiparallel to the spin on site  $i + \delta$ . Both conditions are included in the term  $\vec{S}_i \cdot \vec{S}_{i+\delta} - n_i n_{i+\delta}/4$ . It is interesting to compare this result with the usual  $f$  sum rule. Here the commutator of the current and the polarization in Eq. (34) becomes a commutator of momentum and position, leading to a sum rule depending only on the electron density.

The next-neighbor hopping term in Eq. (41) only contributes for  $x > 0$  and reduces the weight of the UHB in favor of the LHB. In Fig. 4 the nearest-neighbor spin-spin contribution and the three-site hopping contribution

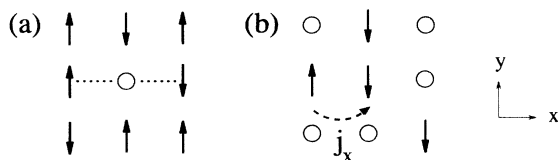


FIG. 3. (a) A hole introduced in the spin background breaks two spin bonds in the  $x$  direction. (b) An excitation to the upper Hubbard band caused by the current operator  $j_x$ .

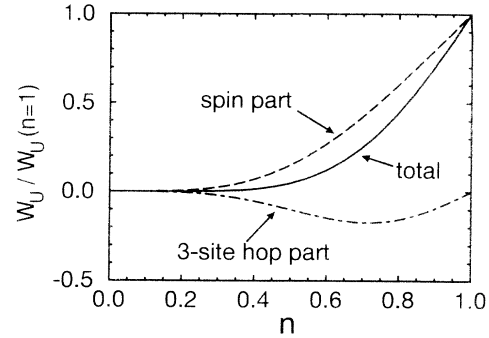


FIG. 4. The spin-spin and three-site hopping contributions to the optical intensity [ $W_U/W_U(x=0)$ ] of the upper Hubbard band in one dimension.

to  $W_U$  [Eq. (47)] are plotted. The three-site hopping term is proportional to  $-x$  for small  $x$ . Therefore, in one dimension for small  $x$ ,  $W_U \simeq (1-3x)W_U(x=0)$ . For  $x \simeq 0.3$  the UHB will have lost already most of its weight.

Because the weight of the UHB depends on the local spin order, its intensity disappears in a sufficiently strong magnetic field. The field dependence of  $W_U$  can be calculated explicitly in one dimension. Adding a Zeeman term to the Hamiltonian will only influence the spin part of the Ogata-Shiba wave function and one finds, for the optical weight of the UHB,

$$W_U = -\frac{4t^2}{U} \left[ n^2 + n \frac{\sin(2\pi n)}{2\pi} - 2 \frac{\sin^2(\pi n)}{\pi^2} \right] \times \left\langle \vec{S}_i \cdot \vec{S}_{i+1} - \frac{1}{4} \right\rangle_{\text{Heisenberg}}, \quad (51)$$

where the spin-spin expectation value depends on the magnetic field. In order to relate this expectation value to the magnetic field we use the result of Ogata, Sugiyama, and Shiba,<sup>46</sup> who showed that the spin system is described by a Heisenberg Hamiltonian,  $H = J_{\text{eff}} \sum_i \vec{S}_i \cdot \vec{S}_{i+1}$ , with an effective exchange,

$$J_{\text{eff}} = \frac{4t^2}{U} n^2 \left( 1 - \frac{\sin(2\pi n)}{2\pi n} \right). \quad (52)$$

The magnetic field dependence of  $\langle \vec{S}_i \cdot \vec{S}_{i+1} \rangle$  was calculated by Griffiths.<sup>47</sup> Combining his tabulated values with the two equations above we obtain Fig. 5. The  $H = 0$  intercept is equal to our previous result for  $W_U$  ( $\langle \vec{S}_i \cdot \vec{S}_{i+1} \rangle = 1/4 - \ln 2$ ). The critical field where the UHB disappears is determined by  $J_{\text{eff}}$ .

The dependence of the optical sum rule of the UHB on the magnetic field might be measured on systems with a sufficiently small exchange constant  $J \simeq 10 - 20$  K. A possible candidate realized in nature is  $\text{CuCl}_2 \cdot 2\text{N}(\text{C}_5\text{D}_5)$ , a 1D antiferromagnet with  $J = 13.4$  K.<sup>48</sup> Although this compound is considered to be an example of the 1D Heisenberg antiferromagnet, the superexchange follows effectively from a 1D Hubbard Hamiltonian. Thus the magnetic field dependence should be as in Fig. 5. Note, however, that because the superexchange is small, the

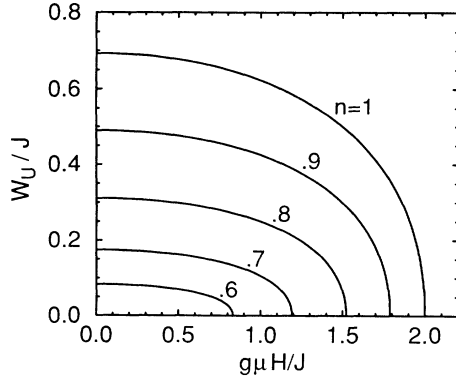


FIG. 5. Spectral weight of the upper Hubbard band, in units of  $J = 4t^2/U$ , as a function of the applied magnetic field  $g\mu H/J$ , for different fillings  $n$ , in one dimension.

intensity of the UHB will be small. Therefore experimentally it might be difficult to identify the UHB or it can become invisible due to other strong (interband) transitions at the same energy (the Hubbard  $U$  value is typically a few eV).

Stephan and Horsch<sup>49</sup> studied the effect of the three-site hopping term in the strong-coupling model on the optical spectrum. They derived a formula for the total oscillator strength, which is equivalent to our Eq. (39) for the LHB. Their numerical results show the importance of the second-order corrections derived above for the spectrum in the LHB. They lead to an increasing Drude weight as well as total weight of the LHB as  $t/U$  increases. In contrast, for the conventional  $t$ - $J$  model both contributions slightly decrease with increasing  $t/U$ .

As an example the optical conductivity for a  $4 \times 3$  cluster with open boundary conditions is shown in Fig. 6. The curves correspond to zero, one, two, and three holes ( $x = 0, 0.08, 0.17$ , and  $0.25$ , respectively). The spectra are averaged over the  $x$  and  $y$  directions. The interband transitions into the UHB ( $\omega > 6t$ ) are seen to be clearly separated from the low-energy intraband transitions for large values of  $U$ . When holes are added, the UHB rapidly loses weight in favor of the LHB. Clearly the LHB has a substantial finite-frequency intensity, in contrast to the 1D clusters. Qualitatively similar results can be obtained using an unrestricted Hartree approach combined with random-phase approximation corrections.<sup>50</sup>

The sum-rule results, Eqs. (45–47), are plotted in Fig. 7. Since the weight at  $n = 1$  is proportional to  $t^2/U$ , there is only little intensity in the UHB for the case  $U = 20$  and the total weight increases rapidly away from half filling. The UHB has already lost most of its intensity when  $n = 0.6$ . The sum-rule expressions are compared with numerical data for ten-site clusters. The total sum rule is obtained by calculating the ground-state expectation value of the kinetic energy. The weight of the UHB is estimated by calculating  $\sigma(\omega)$  like in Fig. 6, splitting the spectrum into LHB and UHB by hand, and integrating the upper part (see also Stephan and Horsch, Ref. 13). The LHB intensity is the difference between the total sum rule and the UHB part. The nice agree-

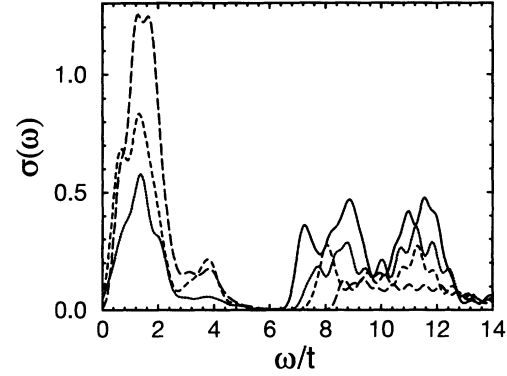


FIG. 6. Optical conductivity  $\sigma(\omega)$  for a 2D  $4 \times 3$  cluster with open boundary conditions. Full, dotted, short-dashed, and long-dashed lines correspond to  $N = 12, 11, 10$ , and  $9$  electrons, respectively. An artificial Gaussian broadening of  $0.5t$  at half width is used.  $U = 10, t = 1$ .

ment between the sum-rule expressions and the ten-site data shows that these clusters are big enough to give an accurate estimate of the sum rules of the infinite chain.

For  $U = 5$  the weight at half filling has increased relative to the weight away from half filling and the total sum rule becomes almost constant in the low doping regime for  $U \simeq W_B$ , where  $W_B$  is the bandwidth. This feature is reproduced by the above sum-rule expressions. The difference between the numerical data and the sum-rule expressions is due to the neglect of higher-order terms. These are especially important for the weight of the UHB.

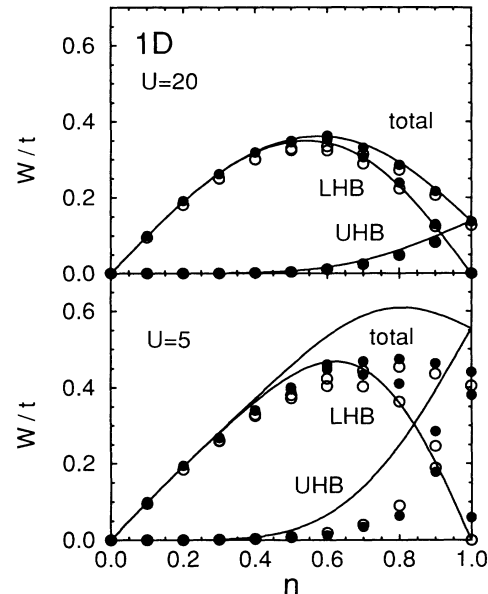


FIG. 7. Total integrated conductivity and partial conductivity of the upper and the lower Hubbard band as a function of the occupation  $n$ , in one dimension, for  $U = 20$  (upper) and  $U = 5$  (lower). The large- $U$  perturbation expansion (lines) is compared with numerical data for a ten-site ring with periodic boundary conditions (full circles) and with open boundary conditions (empty circles).

The figure shows that the weight transfer to the LHB is *enhanced* by the higher-order corrections. Note that the overall optical intensity has increased compared to the  $U = 20$  case<sup>49</sup> due to the second-order terms.

The cluster with open boundary conditions underestimates the weights. This is due to the loss of kinetic energy at the boundary, which is roughly 10% for the ten-site chain. The finite-frequency integral is equal to the expectation value of the kinetic energy. A Drude “precursor” feature is found at finite frequency, the energy of which will go to zero as the system size increases. The periodic boundary conditions give a better estimate of the sum rule. However, the electric response is not well defined for a ring. This, for instance, leads to spurious positive or negative Drude weights at half filling depending on the ring size. The finite-frequency sum is not equal to the kinetic-energy expectation value because part of the weight goes into an  $\omega = 0$  Drude peak.

In Fig. 8 the sum-rule expressions are plotted for the 2D case. Since the ground-state wave function for large  $U$  is not known, the expectation values are calculated from the ground state of the strong-coupling model  $H_{sc}$ , as defined in Eq. (14). The cluster considered is a 2D ten-site cluster with the standard periodic boundaries (see, for instance, Ref. 10). Note that finite-size effects are larger than in the 1D case. This is due to the small diameter of the cluster as well as to the large degeneracy of the one-particle states. The  $N = 6$  particle case has total spin equal to 2 due to this. The ten-site cluster has “accidental” fivefold degeneracies for  $N = 4, 5, 7$ , and 8 electrons. In these cases the results are averaged over the five states. At half filling there is a substantial negative Drude term. Note that the perturbation expression does not show this finite-size effect. The negative Drude weight is due to hopping of the electron all around the torus, so the spurious Drude signal scales like  $(t/U)^L$ , where  $L$  is the diameter of the cluster.<sup>38,51</sup> Therefore the Drude term is higher order in  $t/U$ . Smoother curves can in principle be obtained by optimizing the boundary phases for each number of electrons separately. A  $4 \times 3$  cluster with open

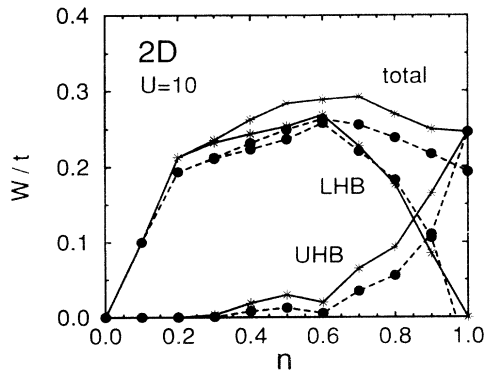


FIG. 8. Same as Fig. 7, but now for two dimensions and  $U = 10, t = 1$ . Numerical data for  $\sqrt{10} \times \sqrt{10}$  Hubbard cluster with periodic boundaries (dots). The sum-rule expressions (stars) are evaluated from the ground-state wave function of the strong-coupling Hamiltonian using the same cluster geometry.

boundaries gives the same qualitative features as the ten-site cluster, but the curves are much smoother and there is no finite Drude weight at half filling. However, a lot of intensity is missing due to the large number of boundary sites. We also compared the sum rules, calculated using the strong-coupling model, with the Hubbard data for  $U = 40$ . The results are in excellent agreement (as they should be) and the expectation values follow all the finite-size irregularities.

As can be seen the qualitative features of the data in two dimensions are the same as in the 1D case. The weight at half filling goes like  $\sim t^2/U$  and the total weight stays roughly constant away from half filling for intermediate- $U$  values. From  $n = 0.2$  to  $n = 1$  the total intensity does not change by more than 30%. This region is much broader than in one dimension due to the different one-particle density of states (DOS). In the 1D model this is peaked at the band edge. Therefore, the particles at the chemical potential in one dimension still have a large kinetic energy for intermediate density and the sum rule increases. In both the 1D and the 2D case, the UHB rapidly loses its intensity away from half filling.

## V. ONE-PARTICLE SPECTRUM: $\vec{k}$ INTEGRATED

In this section we derive expressions for the weights, energy positions, and widths of the UHB and the LHB in the one-particle spectrum. The derivation is analogous to the one presented in the preceding section. Like before all expectation values will be explicitly calculated in one dimension. The  $T = 0$  formalism will be used, but the results are easily extended to finite temperatures  $T \ll U$ .

The local,  $\vec{k}$ -integrated, one-particle spectrum is given by

$$A_{i,\sigma}(\omega) = \sum_f \left| \langle f, N+1 | a_{i,\sigma}^\dagger | 0, N \rangle \right|^2 \times \delta(\omega - (E_f^{N+1} - E_0^N)) + \sum_f \left| \langle f, N-1 | a_{i,\sigma} | 0, N \rangle \right|^2 \times \delta(\omega - (E_0^N - E_f^{N-1})), \quad (53)$$

where  $|f, N \pm 1\rangle$  denotes a many-particle final state with energy  $E_f^{N \pm 1}$  and  $|0, N\rangle$  is the ground state of the  $N$ -particle system. In the above the one-particle spectrum is written explicitly as a sum over an electron addition or inverse photoemission spectroscopy (IPES) part (first term) and an electron removal or photoemission spectroscopy (PES) part (second term). Note that the positive excitation energies in the  $N-1$  spectrum correspond to negative  $\omega$  values. A chemical potential  $\mu_N = (E_0^{N+1} - E_0^{N-1})/2$  can be introduced by replacing  $\omega$  by  $\omega + \mu_N$  on the right-hand side of the above formula. It shifts the total spectrum in such a way that zero energy ( $\omega = 0$ ) lies halfway between the lowest electron-addition and electron-removal state.

The  $n$ th moment of the one-particle spectrum

$$m_{i,\sigma}^{(n)} = \int_{-\infty}^{\infty} A_{\sigma}(\omega) \omega^n d\omega \quad (54)$$

is equivalent to the static expectation value (see, for instance, Ref. 7)

$$m_{i,\sigma}^{(n)} = \left\langle \left\{ a_{i,\sigma}, [H, \dots [H, a_{i,\sigma}^{\dagger}]] \right\} \right\rangle. \quad (55)$$

Curly brackets  $\{ \}$  are used for anticommutators and square brackets  $[ ]$  for commutators. The number of commutators ( $H$  terms) is equal to  $n$ .

The total sum rule or zeroth moment for electron addition plus removal is simply equal to 1. Using the explicit form of the Hamiltonian Eq. (1), the first moment becomes

$$m_{i,\sigma}^{(1)} = U \langle n_{i,\bar{\sigma}} \rangle. \quad (56)$$

In the restricted, translation-symmetric Hartree approximation the one-particle levels with spin  $\sigma$  are shifted upward in energy by an amount  $U \langle n_{\bar{\sigma}} \rangle$ . Since the kinetic part  $T$  of the Hamiltonian (1) is traceless, one finds the same result for the first moment as above, i.e., the mean field gives the correct energy average. The second and higher moments, however, will not be correct since the spread of spectral intensity is grossly underestimated.

The second moment is

$$m_{i,\sigma}^{(2)} = U^2 \langle n_{i,\bar{\sigma}} \rangle + zt^2. \quad (57)$$

The second term on the right-hand side is due to the kinetic energy and is the only term in the restricted Hartree approach. In the Hubbard I approximation,<sup>27</sup> the single dispersive Hartree band is replaced by two bands and the second moment is also conserved (but not the third and higher moments).<sup>52</sup> Equation (57) is therefore consistent with two Hubbard bands, separated by the energy  $U$ , with equal weight (at half filling) and both having the same bandwidth as the  $U = 0$  tight-binding band. A similar picture is obtained from a slave-boson approach including fluctuations.<sup>53</sup>

As before we will express the  $a_{i,\sigma}$  operators in terms of the strong-coupling  $c_{i,\sigma}$  operators. Since the number of doubly occupied sites is then a good quantum number, the moments of the UHB and the LHB can be calculated separately. For the LHB this means [see Eqs. (6), (17), and (18)]

$$m_{i,\sigma;0}^{(0)} = \langle \{ a_{i,\sigma;0}, a_{i,\sigma;0}^{\dagger} \} \rangle, \quad (58)$$

$$\begin{aligned} a_{i,\sigma;0}^{\dagger} &= c_{i,\sigma;0}^{\dagger} - \frac{1}{U} [\tilde{T}_{-U}, c_{i,\sigma;0}^{\dagger}] \\ &+ \frac{1}{U^2} ([[\tilde{T}_{-U}, \tilde{T}_0], c_{i,\sigma;0}^{\dagger}]) \\ &- \frac{1}{2} [\tilde{T}_U, [\tilde{T}_{-U}, c_{i,\sigma;0}^{\dagger}]] \\ &- \frac{1}{2} [\tilde{T}_{-U}, [\tilde{T}_U, c_{i,\sigma;0}^{\dagger}]]. \end{aligned} \quad (59)$$

Evaluation of this sum rule is somewhat tedious, but straightforward. For less than half filling ( $n < 1$ ) there is no double occupancy for  $c$  fermions, so

$$c_{i,\sigma} c_{i,\bar{\sigma}} |0\rangle = 0. \quad (60)$$

With this the expression for the zeroth moment is simplified considerably. The final result is

$$\begin{aligned} \frac{1}{N_a} \sum_{i,\sigma} m_{i,\sigma;0}^{(0)} &= 1 + x + 2 \frac{t}{U} \frac{1}{N_a} \sum_{i,\delta,\sigma} \langle c_{i,\bar{\sigma}}^{\dagger} c_{i+\delta,\bar{\sigma}} \rangle \\ &+ \left( \frac{t}{U} \right)^2 \frac{1}{N_a} \sum_{i,\delta,\delta',\sigma;\delta' \neq \delta} \langle -3c_{i+\delta,\bar{\sigma}}^{\dagger} c_{i+\delta',\bar{\sigma}} \\ &+ 6(c_{i+\delta,\bar{\sigma}}^{\dagger} \tilde{n}_{i,\sigma} c_{i+\delta',\bar{\sigma}} \\ &- c_{i+\delta,\sigma}^{\dagger} c_{i,\bar{\sigma}}^{\dagger} c_{i,\sigma} c_{i+\delta',\bar{\sigma}}) \rangle. \end{aligned} \quad (61)$$

As before,  $x = 1 - n$  is the hole percentage measured from half filling. Since the total number of  $a_{i,\sigma}$  and  $c_{i,\sigma}$  particles is the same,  $\tilde{x} = x$ . The first-order part was derived before by Harris and Lange.<sup>7</sup>

In a similar way it can be shown<sup>7</sup> that  $a_{i,\sigma;2U}^{\dagger}$  and  $a_{i,\sigma;-U}^{\dagger}$  are second order in  $t/U$  and therefore the intensity of the Hubbard bands at  $-U$  and  $2U$  is fourth order in  $t/U$ . This is consistent with the numerical calculations which show that these higher bands have negligible intensity. The intensity of the UHB to second order is therefore

$$\frac{1}{N_a} \sum_{i,\sigma} m_{i,\sigma;U}^{(0)} = 2 - \frac{1}{N_a} \sum_{i,\sigma} m_{i,\sigma;0}^{(0)}. \quad (62)$$

The above expression for the one-particle sum rule of the LHB can be rewritten in terms of the original Fermi operators  $a_{i,\sigma}$ . The first-order term in Eq. (61) leads now to additional second-order terms when transforming the  $c_{i,\sigma}$  operators back to  $a_{i,\sigma}$  fermions. Since there are doubly occupied sites in  $a_{i,\sigma}$  we cannot use the equivalent of Eq. (60) to simplify the final result, but have to start from the full operator expression and keep the  $n_{i\sigma}$  and  $(1 - n_{i\sigma})$  terms

$$\begin{aligned} \frac{1}{N_a} \sum_{i,\sigma} m_{i,\sigma;0}^{(0)} &= 1 + x + 2 \frac{t}{U} \frac{1}{N_a} \sum_{i,\delta,\sigma} \left\langle (1 - n_{i,\sigma}) a_{i,\bar{\sigma}}^{\dagger} a_{i+\delta,\bar{\sigma}} (1 - n_{i+\delta,\sigma}) - n_{i,\sigma} a_{i,\bar{\sigma}}^{\dagger} a_{i+\delta,\bar{\sigma}} n_{i+\delta,\sigma} \right\rangle \\ &+ \left( \frac{t}{U} \right)^2 \frac{1}{N_a} \sum_{i,\delta,\delta',\sigma;\delta' \neq \delta} \left\langle -a_{i+\delta,\bar{\sigma}}^{\dagger} a_{i+\delta',\bar{\sigma}} (3 - 5n_{i+\delta,\sigma} - 5n_{i+\delta',\sigma} + 4n_{i+\delta,\sigma} n_{i+\delta',\sigma}) \right. \\ &+ 6a_{i+\delta,\bar{\sigma}}^{\dagger} n_{i,\sigma} a_{i+\delta',\bar{\sigma}} (1 - n_{i+\delta,\sigma} - n_{i+\delta',\sigma}) - 6a_{i+\delta,\sigma}^{\dagger} a_{i,\bar{\sigma}}^{\dagger} a_{i,\sigma} a_{i+\delta',\bar{\sigma}} (1 - n_{i+\delta,\bar{\sigma}} - n_{i+\delta',\sigma}) \\ &\left. + 2(a_{i+\delta,\bar{\sigma}}^{\dagger} a_{i+\delta',\sigma}^{\dagger} a_{i,\sigma} a_{i,\bar{\sigma}} + a_{i,\bar{\sigma}}^{\dagger} a_{i,\sigma}^{\dagger} a_{i+\delta',\sigma} a_{i+\delta,\bar{\sigma}}) (1 - n_{i+\delta,\sigma} - n_{i+\delta',\bar{\sigma}}) \right\rangle. \end{aligned} \quad (63)$$

The expectation value now has to be evaluated in the ground state of the original Hubbard model. Harris and Lange<sup>7</sup> do not distinguish between  $a_{i\sigma}$  and  $c_{i\sigma}$  operators in the first-order result. This is allowed since all the corrections due to the  $n_{i\sigma}$  and  $(1-n_{i\sigma})$  terms in the first-order expression above are of second order. However, it is well known that the kinetic energy in the Hubbard model is substantial for finite  $t/U$  at half filling [see Eqs. (38) and (45)] and the Harris-Lange first-order term does not vanish, as was also pointed out in Ref. 9. This problem does not occur for the expression in terms of Hubbard operators Eq. (63). It is explicitly electron-hole symmetric and the first- and the second-order term vanish at half filling, and both bands have a weight 1. The  $\sim t/U$  term in Eq. (61) also vanishes since the kinetic energy of the

$c_{i,\sigma}$  fermions is zero at half filling. In first order the total kinetic energy in Eq. (61) is replaced by the difference of the kinetic energy of holes and doubly occupied sites. Note that Eq. (63) is spin-rotationally invariant.

A quantity closer to the XAS experiments is the low-energy electron-addition (IPES) weight. Since the total PES intensity is the number of electrons per site  $n$ , one finds

$$m_{i,\sigma;0}^{(0),\text{IPES}} = m_{i,\sigma;0}^{(0)} - 1 + x. \quad (64)$$

In one dimension the expectation values can again be solved explicitly. From Eq. (61), Eq. (64), and the Ogata-Shiba wave function<sup>35</sup> one obtains, for the IPES weight of the LHB,

$$\sum_{\sigma} m_{i,\sigma;0}^{(0),\text{IPES,1D}} = 2x + \frac{4t}{\pi U} \sin(\pi x) + 6 \left( \frac{t}{U} \right)^2 \left\{ \frac{\sin(2\pi x)}{2\pi} + 2 \ln 2 \left( (1-x) \frac{\sin(2\pi x)}{2\pi} + \frac{\sin^2(\pi x)}{\pi^2} \right) \right\} + \mathcal{O}(t^3/U^3). \quad (65)$$

The first-order term is just the kinetic energy of spinless fermions<sup>54,35</sup> and is obtained by occupying the one-particle levels with one electron each up to the spinless-fermion Fermi wave vector  $k_F = (1-x)\pi$ . The above formula is valid for  $t > 0$ . For negative  $t$  the first-order term will still give a positive contribution to the weight since the expectation value of the kinetic energy will stay negative. In this case the plus sign in the first-order term has to be replaced by a minus sign.

The above results show that in the IPES weight in the LHB at  $U = \infty$  grows twice as fast as the doping and this rapid building up of weight is *enhanced* by  $t$ .<sup>7,8,11,55</sup> The factor 2 is easily understood by counting the available states. At half filling and  $U = \infty$  there are two Hubbard bands separated by  $U$  and there is exactly one particle per site. The total electron-addition weight is equal to the number of unoccupied states and equals  $N_a$ . Similarly, the LHB has a weight equal to the number of particles and equals  $N_a$ . Suppose one removes one particle by means of doping as shown in Fig. 9. Now the number of possible ways to reach the UHB, i.e., to form a double occupation, is  $N_a - 1$  and the UHB loses weight. At the same time there are *two* low-energy addition states since at the site of the removed spin one can add either an up or a down spin without creating a doubly occupied site. For every removed particle we recover two low-energy addition states.

In fact, the above interpretation can be made already using a fully unrestricted Hartree-Fock approximation for large  $U$  (see, for instance, Refs. 56 and 57), which converges to the atomic limit at  $U \rightarrow \infty$ , where the doped holes gain potential energy if they localize on one particular site. This means that for every doped hole one *state* (in contrast to weight) moves down from the UHB to the LHB and there are two low-energy addition states, as in Fig. 9. However, for  $t \neq 0$  the occupation numbers will start to differ from zero or one and the hole states, having

an energy  $\approx U \langle n_{i,\bar{\sigma}} \rangle$ , lie in general somewhere inside the gap; for finite dopings the two bands will tend to merge into one single continuum. Because of this non-integer occupation numbers the total energy spread (UHB and LHB) will be underestimated in the unrestricted Hartree-Fock approximation, except for large  $U$  and close to half filling.

That the effect is enhanced by the hopping  $t$  cannot be understood by a simple counting argument. It is due to interference effects between the ground and the final state. This is illustrated in the simplest way by a two-site Hubbard model with one electron in the ground state (see also Ref. 7). Labeling the sites by 1 and 2, the ground state is the bonding molecular orbital, which for  $t > 0$  takes the form  $|0, N=1\rangle = 1/\sqrt{2}(a_{1,\uparrow}^\dagger + a_{2,\uparrow}^\dagger)|0,0\rangle$ , with  $|0,0\rangle$  being the physical vacuum. Adding a second electron one can reach two low-energy states, a singlet and a triplet. The triplet has energy 0 and its weight is 3/4, independently of the value of  $t$ . The singlet wave function to first order in  $t$  is  $|S, N=2\rangle = |A\rangle + t/U|B\rangle$ , where  $|A\rangle = 1/\sqrt{2}(a_{1,\uparrow}^\dagger a_{2,\downarrow}^\dagger + a_{2,\uparrow}^\dagger a_{1,\downarrow}^\dagger)|0,0\rangle$  and  $|B\rangle =$

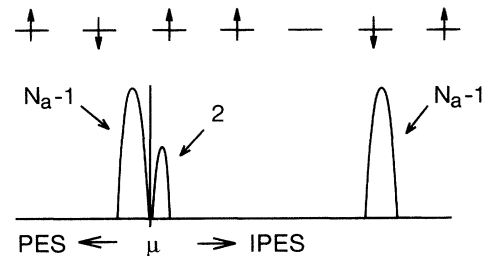


FIG. 9. The one-particle spectrum at  $U = \infty$  for a ground state with one hole in the half-filled band. For every hole introduced two low-energy electron-addition states appear.

$1/\sqrt{2}(a_{1,\uparrow}^\dagger a_{1,\downarrow}^\dagger + a_{2,\uparrow}^\dagger a_{2,\downarrow}^\dagger)|0,0\rangle$ . The weight of this singlet state is  $1/4(1+4t/U)$  and it is enhanced by the hopping. The (positive) sign of the first-order contribution to the weight is the *product* of the + sign of the  $B$  component in the final state and the + sign in the ground state. Since the kinetic energy is directly related to these signs one gets the enhancement of the spectral weight as given by Eq. (61). That the interference between the initial and final states favors the low-energy states is a general phenomenon in valence and core-level spectra of (mixed-valence) compounds where both interactions and hopping are important.<sup>58</sup> Lehner *et al.*<sup>59</sup> gave a qualitative picture of the physical processes leading to the first-order enhancement of the weight in the LHB.

If one neglects the difference between  $a_{i,\sigma}$  and  $c_{i,\sigma}$  fermions (as is usually done), the weight in the  $t$ - $J$  or strong-coupling model is completely determined by the constraint on double occupancy. The weight is now obtained from counting the available states as in Fig. 9 and is independent of  $J$  (or  $t$ ), i.e., the kinetic contribution is completely missing.

In Fig. 10 we schematically draw the electron-addition weight of the LHB as a function of the doping. For  $t=0$  the weight is exactly twice the number of removed particles and this ratio (i.e., the slope of the curve) increases to values between 3 and 4 for small doping  $x$  and  $U$  of the order of the bandwidth.<sup>8</sup> So every removed particle gives rise to 3–4 times as much phase space for adding particles at low energy.

The large- $U$  sum rule in one dimension is compared with numerical estimates of the weight in Fig. 11(a) (see also Ref. 11 for more details). Only the kinetic contribution to the weight is plotted, i.e., the linear term  $\sim 2x$  (state-counting part) is subtracted from curves like the one shown in Fig. 10. For comparison the first-order spinless fermion term is shown for  $U=5$ . As can be seen the expectation values in Eq. (63) are close to the results for infinite system obtained from the Ogata-Shiba wave function<sup>35</sup> for the strong-coupling model, even for intermediate- $U$  values. The second-order term enhances the weight for occupation numbers near half filling and corrects the weight overestimated in first order for small fillings. As seen in Fig. 11(a), for  $U$  of the order of the

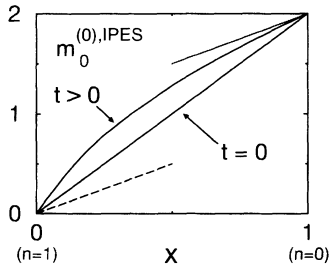


FIG. 10. Schematic drawing of the increase of the low-energy electron-addition spectral weight (or zeroth moment of the inverse-photoemission intensity in the lower Hubbard band) as a function of the doping  $x$  away from half filling due to the hopping  $t$ . The lower dashed line would follow for a semiconductor and the upper dotted line is the limit of no intensity in the upper band for the almost empty (almost filled) band.

bandwidth ( $U=5$ ), the second-order term overestimates the extra kinetic weight by not more than 30%.

Figure 11(b) shows representative results for two dimensions as obtained from the  $\sqrt{10} \times \sqrt{10}$  cluster with periodic boundaries which was also used for the optical conductivity in Sec. IV. The kinks occurring for  $N=2$  and 6 electrons are a finite-size effect and reflect the one-particle level structure. We found that the first-order kinetic energy term is well described using spinless fermions in two dimensions.<sup>60</sup> As shown in a previous paper,<sup>11</sup> the results are very similar to the 1D case and the agreement is even quantitative if one scales the hopping inversely proportionally to the square root of the dimension. Notice that the perturbation results show the same finite-size kinks as the integrated spectra.

Expressions for the energy position and width of the two Hubbard bands can be obtained in a similar way. They are related to the first and second moments of the individual bands. The (local) first moments of the LHB and UHB are defined as

$$m_{i,\sigma;0}^{(1)} = \left\langle \left\{ [a_{i,\sigma;0}, H], a_{i,\sigma;0}^\dagger \right\} \right\rangle, \quad (66)$$

$$m_{i,\sigma;U}^{(1)} = \left\langle \left\{ [a_{i,\sigma;-U}, H], a_{i,\sigma;U}^\dagger \right\} \right\rangle. \quad (67)$$

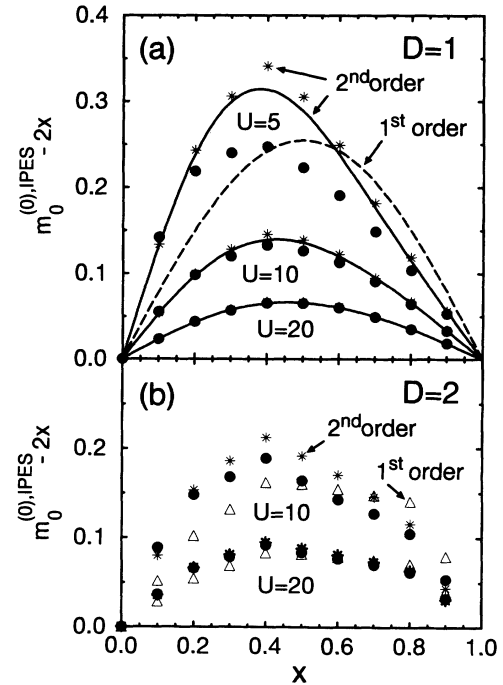


FIG. 11. Kinetic part of the low-energy electron-addition weight as a function of the doping  $x$  in (a) one and (b) two dimensions ( $t=1$ ). The second-order result Eq. (65) [line in (a)] is compared with numerical results (filled dots) for the one-particle spectrum of a ten-site ring. As a check the second-order weight is also calculated from Eq. (63) (stars) using the numerical ground state of the ten-site Hubbard ring and the  $\sqrt{10} \times \sqrt{10}$  cluster, respectively. The dashed line in (a) shows the first-order contribution for  $U=5$ , while the triangles in (b) are the perturbation results to first order only.

Using  $H = \tilde{V} + \tilde{T}_0 + \mathcal{O}(t^2/U)$  and  $[a_{i,\sigma,-U}, \tilde{V}] = U a_{i,\sigma,-U}$ , we find to lowest order, for the energy difference between the UHB and LHB,

$$\begin{aligned} E^{\text{UHB}} - E^{\text{LHB}} &= \frac{\sum_{i,\sigma} m_{i,\sigma;U}^{(1)}}{\sum_{i,\sigma} m_{i,\sigma;U}^{(0)}} - \frac{\sum_{i,\sigma} m_{i,\sigma;0}^{(1)}}{\sum_{i,\sigma} m_{i,\sigma;0}^{(0)}} \\ &= U + \frac{2xt}{(1-x)(1+x)} \frac{1}{N_a} \sum_{i,\delta,\sigma} \langle c_{i,\bar{\sigma}}^\dagger c_{i+\delta,\bar{\sigma}} \rangle \\ &\quad + \mathcal{O}(t^2/U). \end{aligned} \quad (68)$$

In one dimension spinless fermions give

$$\begin{aligned} E^{\text{UHB,1D}} - E^{\text{LHB,1D}} \\ = U + \frac{4xt}{(1-x)(1+x)\pi} \sin(\pi x) + \mathcal{O}(t^2/U). \end{aligned} \quad (69)$$

This quantity is plotted in Fig. 12(a). The interband separation *increases* from  $U$  at half filling to  $U + 2t$  in the (almost) empty band case. The  $n \rightarrow 0$  limit can be understood in the following way. Suppose there is just one electron with energy  $-2t$ . Then, if we add an electron to the LHB it will be independent of the first and will have an energy between  $-2t$  and  $2t$ . As a result the total final-state energy lies between  $-4t$  and  $0$ . To reach the UHB the particle has to form a bound state with the first electron. This may be realized only if the first particle loses its kinetic energy since the dispersion of the bound state is only of order  $t^2/U$ .<sup>61</sup> Consequently, the total UHB energy is  $U$  and the band separation  $U + 2t$ . For finite densities there is a finite probability that the doubly occupied site has a singly occupied site as a neighbor. The UHB dispersion becomes of order  $t$  and the band sep-

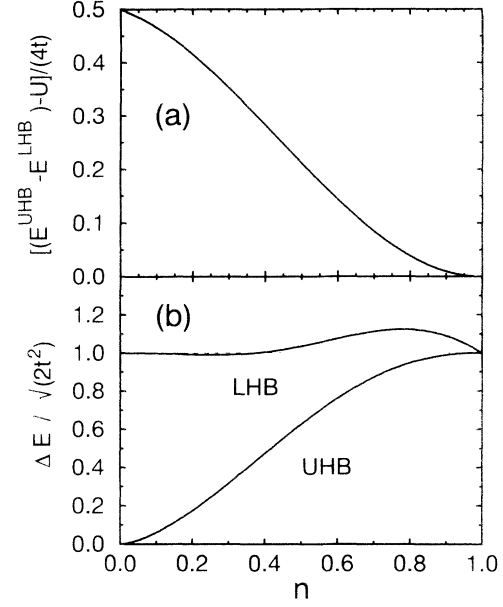


FIG. 12. (a) Energy separation of the two Hubbard bands and (b) the width of the lower and the upper band (b) in one dimension, as a function of the density  $n = 1 - x$ .

aration decreases to  $U$  at half filling (see also Ref. 55). One can expect that for hole doping the distance between the bands increases further beyond the term  $\sim t$  due to second-order contributions  $\sim t^2/U$ . This occurs because away from half filling the  $(N + 1)$  states of the LHB and the  $(N - 1)$  states of the UHB states hybridize, as in the above two-site example. An increasing distance is indeed observed as a function of doping in the XAS and EELS spectra.<sup>1,2</sup>

In a similar way one finds, for the width of the UHB,

$$\begin{aligned} (\Delta E^{\text{UHB}})^2 &= \frac{\sum_{i,\sigma} m_{i,\sigma;U}^{(2)}}{\sum_{i,\sigma} m_{i,\sigma;U}^{(0)}} - \left( \frac{\sum_{i,\sigma} m_{i,\sigma;U}^{(1)}}{\sum_{i,\sigma} m_{i,\sigma;U}^{(0)}} \right)^2 \\ &= zt^2 + t^2 \frac{1}{1-x} \frac{1}{N_a} \sum_{i,\delta,\delta',\sigma;\delta \neq \delta'} \langle c_{i+\delta,\bar{\sigma}}^\dagger (1 - \tilde{n}_i) c_{i+\delta',\bar{\sigma}} \rangle - t^2 \left( \frac{1}{1-x} \frac{1}{N_a} \sum_{i,\delta,\sigma} \langle c_{i,\bar{\sigma}}^\dagger c_{i+\delta,\bar{\sigma}} \rangle \right)^2 + \mathcal{O}(t^3/U) \end{aligned} \quad (70)$$

and, for the LHB,

$$\begin{aligned} (\Delta E^{\text{LHB}})^2 &= zt^2 + \frac{t^2}{1+x} \frac{1}{N_a} \sum_{i,\delta,\delta',\sigma;\delta \neq \delta'} \langle -c_{i+\delta,\bar{\sigma}}^\dagger \tilde{n}_i c_{i+\delta',\bar{\sigma}} + 2(c_{i+\delta,\bar{\sigma}}^\dagger \tilde{n}_i c_{i+\delta',\bar{\sigma}} - c_{i+\delta,\sigma}^\dagger c_{i,\bar{\sigma}} c_{i+\delta',\sigma}) \rangle \\ &\quad - \left( \frac{t}{1+x} \frac{1}{N_a} \sum_{i,\delta,\sigma} \langle c_{i,\bar{\sigma}}^\dagger c_{i+\delta,\bar{\sigma}} \rangle \right)^2 + \mathcal{O}(t^3/U). \end{aligned} \quad (71)$$

Following the reasoning above, one expects that the width of the UHB to order  $t$  vanishes as  $n \rightarrow 0$  and that the width of the LHB becomes equal to the free-particle bandwidth. Estimating the expectation values above for

$n \rightarrow 0$  one finds this result independently of the dimension. At half filling the expectation values in Eqs. (70) and (71) vanish since they are related to  $c_{i,\sigma}$  fermions and the site indices are different. Now the bandwidth of each

of the Hubbard bands is equal to that of free particles ( $U = 0$ ) and there is no overall band narrowing to order  $t$ . This is consistent with the results of Brinkman and Rice,<sup>62</sup> who found that the *edge to edge* distance of the LHB is reduced, but at the same time there is a piling-up of weight close to the edge such that the second moment is unaffected.

The expectation values consist again of kinetic-energy and three-site hopping terms. As before one can use the Ogata-Shiba wave function to evaluate the above equations in one dimension,

$$(\Delta E^{\text{UHB}})^2 = 2t^2 \left[ 1 + (1-n) \frac{\sin(2\pi n)}{2\pi n} - (2-n) \frac{\sin^2(\pi n)}{(\pi n)^2} \right] + \mathcal{O}(t^3/U), \quad (72)$$

$$(\Delta E^{\text{LHB}})^2 = 2t^2 \left[ 1 - \frac{2}{(2-n)^2} \frac{\sin^2(\pi n)}{\pi^2} - \frac{2 \ln 2 + 1}{2-n} \left( n \frac{\sin(2\pi n)}{2\pi} - \frac{\sin^2(\pi n)}{\pi^2} \right) \right] + \mathcal{O}(t^3/U). \quad (73)$$

Equations (72) and (73) are plotted in Fig. 12(b).

Because we frequently used the fact that there are no doubly occupied  $c_{i,\sigma}$  sites, the above formulas do not seem to be electron-hole symmetric. But in fact they are. This can be demonstrated explicitly by writing the expressions in terms of the original  $a_{i\sigma}$  operators, like in Eq. (63), which gives rise to extra  $n_{i,\sigma}$  and  $1-n_{i,\sigma}$  terms.

## VI. TWO-POLE APPROACH AND MOMENTUM DEPENDENCE OF THE ONE-PARTICLE SPECTRUM

In this section a comparison is made between the perturbation theory and the non-perturbative two-pole ansatz for the one-particle spectrum. In this latter approach the aim is to find the best possible approximation to the  $\vec{k}$  dependent one-particle spectrum using two  $\delta$  functions, with their energies and weights dependent on  $\vec{k}$ . Making this ansatz, the best approximation is achieved if the first four moments of the spectral density are conserved, as postulated by Roth in 1969.<sup>52</sup> Since then this approach to the one-particle spectrum has been studied by many authors<sup>52,63–66</sup> and became a general method to treat approximately the spectral density in an interacting system without a small parameter.<sup>67–73</sup> For the Hubbard model this approach can be viewed as an improved Hubbard I approximation. It is also closely related to the numerical Lanczos technique and is equivalent to the first two steps of the corresponding continued fraction. Because the method makes use of the first couple of moments it is closely related to the perturbation theory described above and we will clarify the similarities between both approaches. As we will see below the two-pole approach has the advantage that it describes the  $\vec{k}$

dependence of the spectra more accurately than the perturbation theory for intermediate or even large values of  $U$ .

Consider two poles (labeled 1 and 2) with the corresponding weights  $w_{1(2),\vec{k},\sigma}$  and energies  $\varepsilon_{1(2),\vec{k},\sigma}$ . They are related to the  $n$ th moment ( $n = 0, \dots, 3$ ) of the  $\vec{k}$ -dependent one-particle spectrum by

$$w_{1,\vec{k},\sigma} \varepsilon_{1,\vec{k},\sigma}^n + w_{2,\vec{k},\sigma} \varepsilon_{2,\vec{k},\sigma}^n = m_{\vec{k},\sigma}^{(n)}. \quad (74)$$

The moments are most conveniently evaluated in real space using the Fourier decomposition of  $a_{\vec{k},\sigma}$ . Using Eq. (55), the first four moments are<sup>64</sup>

$$\begin{aligned} m_{\vec{k},\sigma}^{(0)} &= 1, \\ m_{\vec{k},\sigma}^{(1)} &= U n_{\bar{\sigma}} + \varepsilon_{\vec{k}}, \\ m_{\vec{k},\sigma}^{(2)} &= U^2 n_{\bar{\sigma}} + 2U \varepsilon_{\vec{k}} n_{\bar{\sigma}} + \varepsilon_{\vec{k}}^2, \\ m_{\vec{k},\sigma}^{(3)} &= U^3 n_{\bar{\sigma}} + U^2 \left[ (2n_{\bar{\sigma}} + n_{\bar{\sigma}}^2) \varepsilon_{\vec{k}} + B_{\vec{k},\sigma} \right] \\ &\quad + 3U \varepsilon_{\vec{k}}^2 n_{\bar{\sigma}} + \varepsilon_{\vec{k}}^3, \end{aligned} \quad (75)$$

where  $n_{\bar{\sigma}} = (1/N_a) \sum_i \langle n_{i,\bar{\sigma}} \rangle$ ,  $\varepsilon_{\vec{k}}$  is the one-particle dispersion defined by Eq. (30), and

$$\begin{aligned} B_{\vec{k},\sigma} &= \frac{t}{N_a} \sum_{i,\delta} \langle (1-n_{i,\sigma}) a_{i,\bar{\sigma}}^\dagger a_{i+\delta,\bar{\sigma}} (1-n_{i+\delta,\sigma}) \\ &\quad - n_{i,\sigma} a_{i,\bar{\sigma}}^\dagger a_{i+\delta,\bar{\sigma}} n_{i+\delta,\sigma} \rangle \\ &\quad + \varepsilon_{\vec{k}} \langle (n_{i,\bar{\sigma}} n_{i+\delta,\bar{\sigma}}) - (a_{i,\sigma}^\dagger a_{i+\delta,\bar{\sigma}}^\dagger a_{i,\bar{\sigma}} a_{i+\delta,\sigma}) \rangle \\ &\quad - n_{\bar{\sigma}}^2 - \langle a_{i,\sigma}^\dagger a_{i,\bar{\sigma}}^\dagger a_{i+\delta,\bar{\sigma}} a_{i+\delta,\sigma} \rangle. \end{aligned} \quad (76)$$

Here we assumed that the expectation values are site independent. The term proportional to  $t$  is *local*, i.e.,  $\vec{k}$  independent. It is similar to the first-order term in Eq. (63) and describes the difference of the kinetic energies of holes and doubly occupied sites. The second term for a large part determines the  $\vec{k}$  dependence of the pole energies. The first two expectation values of the second term combine to a nearest-neighbor spin correlation function, showing that the dispersion of the peaks is directly influenced by the spin order. The last expectation value involves the hopping of a double occupancy and is small for large and intermediate  $U$ . This latter term is of importance for the negative- $U$  Hubbard model.

The solution of the above equations is<sup>64</sup>

$$\begin{aligned} \varepsilon_{1(2),\vec{k},\sigma} &= \frac{1}{2} [U + \varepsilon_{\vec{k}} + \beta_{\vec{k},\sigma} \\ &\quad \pm \sqrt{(U - \varepsilon_{\vec{k}} + \beta_{\vec{k},\sigma})^2 + 4U n_{\bar{\sigma}} (\varepsilon_{\vec{k}} - \beta_{\vec{k},\sigma})}], \\ w_{1,\vec{k},\sigma} &= \frac{U(1-n_{\bar{\sigma}}) + \beta_{\vec{k},\sigma} - \varepsilon_{1,\vec{k},\sigma}}{\varepsilon_{2,\vec{k},\sigma} - \varepsilon_{1,\vec{k},\sigma}}, \\ w_{2,\vec{k},\sigma} &= 1 - w_{1,\vec{k},\sigma}, \end{aligned} \quad (77)$$

and  $\beta_{\vec{k},\sigma} = [n_{\bar{\sigma}}(1-n_{\bar{\sigma}})]^{-1} B_{\vec{k},\sigma}$ , with  $n_{\bar{\sigma}} = (1/N_a) \sum_i \langle n_{i,\bar{\sigma}} \rangle$ . If one sets  $B_{\vec{k},\sigma} = 0$  in the above, the derived equations are identical to those obtained in the

Hubbard I approximation.<sup>27</sup> As Hubbard showed, this approximation becomes exact in the limits  $U = 0$  and  $U \rightarrow \infty$ . However, concerning the weights of the UHB and the LHB the approximation is very poor for finite  $t$  and predicts a *decrease* of the weight of the LHB for fillings smaller than  $n = 1$ .<sup>11</sup> In the Hubbard I approximation the dispersion is completely determined by  $\epsilon_{\vec{k}}$  and both bands have a more or less similar shape  $\sim \cos k$  in one dimension for all fillings. On the contrary, numerical calculations show that the first moments of the UHB and the LHB have a much richer behavior as a function of  $U$  and the filling  $n$ .<sup>10,66</sup> The  $\vec{k}$ -independent part of  $B_{\vec{k},\sigma}$  corrects the weights of the bands as compared to the Hubbard I approximation and shifts the bands.<sup>7,64</sup> The  $\vec{k}$ -dependent part is essential for the “dispersion” of the energies of the two peaks.<sup>66</sup>

Using again the Ogata-Shiba wave function,<sup>35</sup> one finds in one dimension, for large  $U$ ,

$$\begin{aligned} B_{k,\sigma} &\approx \frac{t}{N_a} \sum_{i,\sigma} \langle c_{i,\sigma}^\dagger c_{i+1,\sigma} \rangle \\ &+ \epsilon_k \left( \langle \vec{S}_i \cdot \vec{S}_{i+1} + \frac{1}{4} \tilde{n}_i \tilde{n}_{i+1} \rangle - \frac{n^2}{4} \right) \\ &= t \frac{\sin(\pi n)}{\pi} - \epsilon_k \left[ \frac{n^2}{4} - \left( \frac{1}{2} - \ln 2 \right) \right. \\ &\quad \left. \times \left( n^2 - \frac{\sin^2(\pi n)}{\pi^2} \right) \right]. \end{aligned} \quad (78)$$

The two-pole approach can now be compared with the perturbation approach. Repeating the calculation in Sec. V for the  $\vec{k}$ -dependent spectrum, one finds (see also Ref. 7)

$$\begin{aligned} m_{\vec{k},\sigma,0}^{(0)} &= 1 - n_{\bar{\sigma}} + \frac{2t}{U} \frac{1}{N_a} \sum_{i,\delta} \langle (1 - n_{i,\sigma}) a_{i,\bar{\sigma}}^\dagger a_{i+\delta,\bar{\sigma}} (1 - n_{i+\delta,\sigma}) - n_{i,\sigma} a_{i,\bar{\sigma}}^\dagger a_{i+\delta,\bar{\sigma}} n_{i+\delta,\sigma} \rangle \\ &\quad - \frac{2\epsilon_{\vec{k}}}{U} \left( n_{\bar{\sigma}} - \langle n_{i,\bar{\sigma}} n_{i+\delta,\bar{\sigma}} \rangle + \langle a_{i,\sigma}^\dagger a_{i+\delta,\bar{\sigma}}^\dagger a_{i,\bar{\sigma}} a_{i+\delta,\sigma} \rangle + \langle a_{i,\sigma}^\dagger a_{i,\bar{\sigma}}^\dagger a_{i+\delta,\bar{\sigma}} a_{i+\delta,\sigma} \rangle \right) + \mathcal{O}(t^2/U^2) \\ &= 1 - \tilde{n}_{\bar{\sigma}} + \frac{2t}{U} \frac{1}{N_a} \sum_{i,\delta} \langle c_{i,\bar{\sigma}}^\dagger c_{i+\delta,\bar{\sigma}} \rangle - \frac{2\epsilon_{\vec{k}}}{U} \left( \tilde{n}_{\bar{\sigma}} - \langle \tilde{n}_{i,\bar{\sigma}} \tilde{n}_{i+\delta,\bar{\sigma}} \rangle + \langle c_{i,\sigma}^\dagger c_{i+\delta,\bar{\sigma}}^\dagger c_{i,\bar{\sigma}} c_{i+\delta,\sigma} \rangle \right) + \mathcal{O}(t^2/U^2) \end{aligned} \quad (79)$$

and the energy average is

$$\begin{aligned} E_{\vec{k},\sigma}^{\text{LHB}} &= m_{\vec{k},\sigma,0}^{(1)} / m_{\vec{k},\sigma,0}^{(0)} \\ &= \frac{\epsilon_{\vec{k}}}{1 - n_{\bar{\sigma}}} \left( 1 - 2n_{\bar{\sigma}} + \langle n_{i,\bar{\sigma}} n_{i+\delta,\bar{\sigma}} \rangle - \langle a_{i,\sigma}^\dagger a_{i+\delta,\bar{\sigma}}^\dagger a_{i,\bar{\sigma}} a_{i+\delta,\sigma} \rangle - \langle a_{i,\sigma}^\dagger a_{i,\bar{\sigma}}^\dagger a_{i+\delta,\bar{\sigma}} a_{i+\delta,\sigma} \rangle \right) \\ &\quad + \frac{t}{1 - n_{\bar{\sigma}}} \frac{1}{N_a} \sum_{i,\delta} \langle (1 - n_{i,\sigma}) a_{i,\bar{\sigma}}^\dagger a_{i+\delta,\bar{\sigma}} (1 - n_{i+\delta,\sigma}) - n_{i,\sigma} a_{i,\bar{\sigma}}^\dagger a_{i+\delta,\bar{\sigma}} n_{i+\delta,\sigma} \rangle + \mathcal{O}(t^2/U). \end{aligned} \quad (80)$$

Summing over the spin index

$$\begin{aligned} E_{\vec{k}}^{\text{LHB}} &= \frac{2\epsilon_{\vec{k}}}{2-n} (1 - n + \langle \vec{S}_i \cdot \vec{S}_{i+\delta} + \frac{1}{4} \tilde{n}_i \tilde{n}_{i+\delta} \rangle) \\ &\quad + \frac{t}{2-n} \frac{1}{N_a} \sum_{i,\delta,\sigma} \langle c_{i,\bar{\sigma}}^\dagger c_{i+\delta,\bar{\sigma}} \rangle + \mathcal{O}(t^2/U). \end{aligned} \quad (81)$$

Taylor expansion of the two-pole expression Eq. (77) for small  $(t/U)$  leads to the same result. Therefore the two approaches are identical to first order in  $t/U$ . The second-order weight, however, was shown to depend on next-nearest-neighbor expectation values [see Eq. (61)]. In the two-pole approach only nearest-neighbor terms appear. Therefore the two poles in the two-pole approach represent the two Hubbard bands *only* to first order in  $t/U$ . Although this approach is nonperturbative, one can no longer strictly identify the two poles with the two Hubbard bands for intermediate  $t/U$  and for noninteger filling. It is clear from the above that the lower pole in the two-pole approach should not be interpreted as a quasiparticle, but as the average of the one-particle spectrum over the LHB.<sup>74</sup> As such it stands for both the coher-

ent and incoherent contributions (if we can talk about Fermi-liquid quasiparticles at all).

The expectation values occurring in the  $\vec{k}$ -independent part of  $B_{\vec{k},\sigma}$  can be calculated from the Green's functions. This then leads to a set of self-consistent equations. For the  $\vec{k}$ -dependent part, however, this is not possible. Therefore this term is often treated by a Hartree decoupling, or even totally neglected, using the argument that its physical consequences are insignificant.<sup>64,65</sup> It is clear from Eq. (81), however, that this term is crucial for the correct  $\vec{k}$  dependence of the two poles. One finds that the average band dispersion around half filling is determined by the nearest-neighbor spin correlation function. Mehlig *et al.*<sup>66</sup> have shown that the decoupling proposed by Roth<sup>52</sup> gives a good approximation of these expectation values and describes the large doping-dependent changes of the dispersion close to half filling.

The same two-pole approach can also be worked out in real space. This means that the entire spectrum is approximated by only two poles instead of two per  $\vec{k}$  value. The resulting expressions are directly obtained

from Eqs. (75) and (76) by replacing odd powers of  $\epsilon_{\vec{k}}$  by 0 and  $\epsilon_{\vec{k}}^2$  by  $zt^2$ , respectively. In this  $\vec{k}$ -independent case the comparison with the two Hubbard bands is much worse and shows that the two-pole ansatz is meaningful only close to half filling.<sup>60</sup> For small electron densities the two poles will try to describe the width of the LHB instead of the distance between the two Hubbard bands. Therefore, for  $n \rightarrow 0$  one finds that the upper pole has a weight 1/2 and lies in the LHB. On the contrary, the  $\vec{k}$ -dependent two-pole approach gives the correct behavior for  $n \rightarrow 0$ . The weight of the upper pole now vanishes in this limit. Therefore the  $\vec{k}$ -dependent approach is superior even if one wants to describe only  $\vec{k}$ -integrated properties.

In one dimension for large  $U$  one finds

$$E_k^{\text{LHB,1D}} = \frac{-4t \cos k}{2-n} \left[ 1 - n + \left( \frac{1}{2} - \ln 2 \right) \times \left( n^2 - \frac{\sin^2(\pi n)}{\pi^2} \right) \right] + \frac{2t}{\pi(2-n)} \sin(\pi n) + \mathcal{O}(t^2/U), \quad (82)$$

$$m_{k;0}^{(0),1D} = \sum_{\sigma} m_{k,\sigma;0}^{(0),1D} = 2 - n + \frac{4t}{\pi U} \sin(\pi n) + \frac{4t \cos k}{U} \left[ n - (1 - 2 \ln 2) \left( n^2 - \frac{\sin^2(\pi n)}{\pi^2} \right) \right] + \mathcal{O}(t^2/U^2), \quad (83)$$

which is consistent with Eqs. (31) and (65). In the above expressions the “average dispersion” is proportional to  $\epsilon_{\vec{k}}$ ,  $E_k^{\text{LHB,1D}} \simeq A\epsilon_{\vec{k}} + \text{const}$ . We would like to stress that this quantity is just the average over the LHB,<sup>74</sup> in contrast to the quasiparticle states at low energy, which describe the coherent propagation at large  $U$ .<sup>75</sup> The dispersion coefficient  $A$  is displayed in Fig. 13. One finds a crossover for a filling  $n \approx 0.86$ , where the dispersion changes its sign. Consequently, at half filling the  $k = 0$  point has a lower average binding energy than the  $k = \pi$  point. From Eq. (81) it follows that this dispersion vanishes at half filling for a Néel ordering of the spins, which is consistent with the retraceable-path approach.<sup>62</sup> Instead, for a random or ferromagnetic spin order the dispersion is not reversed, independently of the dimension.

Before showing the results for the two-pole approach, we will focus on the features seen in numerical simulations.<sup>10,12,66</sup> The numerically obtained excitation spectra show various interesting features. At half filling for finite  $U$  the minimum excitation energy lies at  $\pi/2$ , the  $U = 0$  Fermi point. The lowest binding energy peak between  $k = 0$  and  $k = \pi/2$  shows very little dispersion for large  $U$ , while the part between  $\pi/2$  and  $\pi$  is strongly  $k$  dependent. The width of the band is small at  $k = 0$  and  $k = \pi$  and large at  $k = \pi/2$ . For just one hole in, say, a ten-site cluster (corresponding to  $\sim 10\%$  doping) this behavior changes drastically. Weight appears in the low-energy electron-addition spectrum for *all*  $k > k_F$  points and the spectrum shows a large, Luttinger-like, Fermi

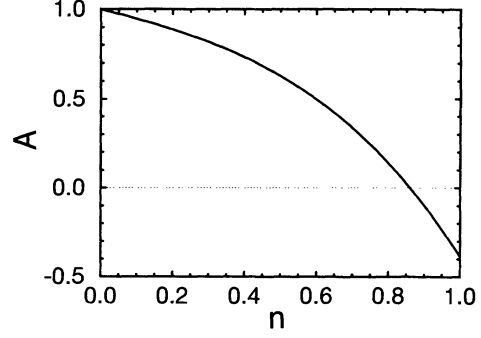


FIG. 13. Dispersion coefficient  $A$  of the first moment of the lower Hubbard band in one dimension ( $E_k^{\text{LHB}} = A\epsilon_k + \text{const}$ ) as a function of the density  $n$ .

surface.<sup>76</sup> The weight for these  $k$  points grows steadily as the doping is increased. For  $k$  points inside the Luttinger volume there is almost no low-energy electron-addition weight for any filling. The “dispersion” changes to the usual cosine form with a bandwidth which increases when the doping is increased. Note that the two-pole approach must be compared with the weighted average over the spectra. This average energy also changes quickly with doping. In the 1D cluster of ten sites used for numerical evaluation we observed the change from a reversed behavior at half filling via practically flat dispersion for one hole added to the normal  $\sim \cos k$  band for more than one hole. The transferred weight from the UHB to the LHB is distributed over *all*  $k$  points with  $k > k_F$ , not just over the ones at  $k_F$ . A similar behavior of the  $k$ -dependent spectra is found in the  $t$ - $J$  model and the above features are qualitatively similar in two dimensions.

In Fig. 14 the  $k$ -dependent energy of the lower pole is shown for three different fillings. The two-pole results are calculated using Eqs. (77) and (78). As pointed out above, the rather flat dispersion close to half filling changes into a broader band with increasing doping (note the different scale for  $n = 0.6$ ). The numerical data points are weighted energy averages over the LHB only, obtained by splitting the one-particle spectra into the UHB and the LHB by hand. For  $n = 0.6$  the LHB shows the normal cosine dispersion with a reduced “width” with respect to the free dispersion at  $n = 0$  (see also Fig. 13). The two-pole result reproduces the numerical data very well, even for  $U = 5$ . For  $n = 0.9$  both the numerical energy average and the lower pole become almost dispersionless. For smaller- $U$  values the two-pole approach is not sufficiently accurate to follow the fast changes in the spectra compared to the half-filled case. Finally, for very large values of  $U$  the picture has changed drastically at half filling and the dispersion is a reversed cosine, with the lowest energy at  $k = \pi$  [see Eq. (81)]. However, with decreasing  $U$  the energy of the  $k = 0$  pole decreases and the  $k = \pi/2$  pole has the highest kinetic energy or the lowest binding energy. The numerical and two-pole results are in good agreement, apart from the “kink” at  $\pi/2$ , which is not reproduced by the two-pole ansatz (this might be a finite-size effect). The results show that the two-pole approach describes the  $k$  dependence much bet-

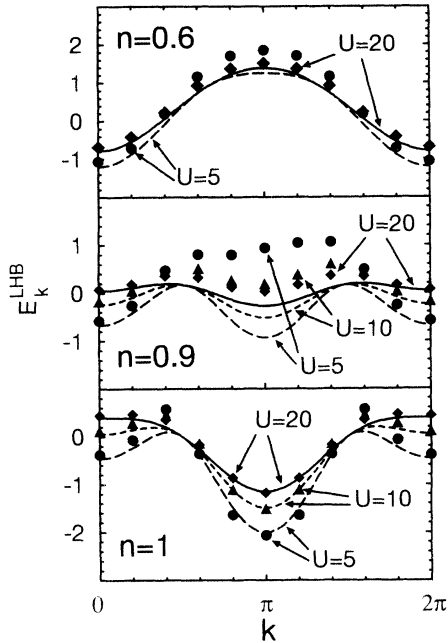


FIG. 14. Momentum-dependent average energy of the lower Hubbard band  $E_k^{\text{LHB}}$  for  $U = 5, 10$ , and  $20$  ( $t = 1$ ), at half filling (lower), for 10% doping (middle) and 40% doping (upper part). Symbols are numerical data for a ten-site cluster and lines represent the results of the two-pole approach combined with the Ogata-Shiba wave function (Ref. 35).

ter for smaller- $U$  values than first-order perturbation theory. Deviations from the first-order cosine behavior are appreciable and even qualitative differences occur already for  $U = 10$ . It is apparent that a double unit-cell mean-field antiferromagnetic dispersion does not describe the spectra at half filling.

It is clear from Eq. (81) that the above features are a direct consequence of the spin order. At half filling Brinkman and Rice<sup>62</sup> showed that for a Néel ground state the spectrum becomes completely  $k$  independent. This is, however, an artifact of the static spin order. If quantum spin fluctuations are included as in the Ogata-Shiba wave function,<sup>35</sup> the spectra become strongly  $k$  dependent and the above features are obtained.<sup>77-79</sup>

The behavior of the  $k$ -dependent weight is displayed in Fig. 15. In Fig. 15(a) the weight of the lower pole at half filling is plotted. Since this consists purely of electron-removal states it is equal to the occupation number  $n_k$ . A comparison with Fig. 2 shows that the two-pole approach is again superior over first-order perturbation theory and reproduces quite well the  $k$  dependence of  $n_k$  down to  $U = 5$  at half filling. Note that we used the large- $U$  Ogata-Shiba wave function to calculate the pole weights.

The momentum-dependent increase of the weight in the LHB, displayed in Fig. 15(b), is more sensitive to the hole dynamics at finite  $U$ . The slight asymmetry in  $k$  is due to the finite momentum of the one-hole ground state of the cluster. The numerical data represent the weight of the LHB at half filling subtracted from the weight as obtained for the one-hole ground state. In case of the two-pole approach we took the difference between the

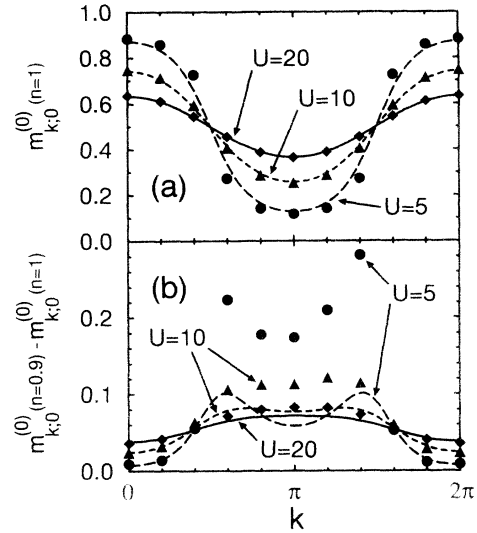


FIG. 15. (a)  $k$ -dependent weight of the lower Hubbard band  $m_{k;0}^{(0)}$  (equal to  $n_k$ ) at half filling ( $n = 1$ ) and (b)  $k$  dependence of the weight transfer from the upper to the lower band  $m_{k;0}^{(0)}(n = 0.9) - m_{k;0}^{(0)}(n = 1)$  in one dimension. Symbols stand for numerical data for a ten-site cluster for three values of  $U$  ( $t = 1$ ). Lines are the two-pole approach combined with the Ogata-Shiba wave function (Ref. 35).

weight of the lower pole for  $n = 0.9$  and  $n = 1$ . For large  $U$  the weight increase distributes over all  $k$  values. However, for smaller- $U$  values the weight is mainly distributed over  $k$  states larger than but still close to  $k_F$ . Again one finds that the two- $\delta$ -function ansatz is not able to follow the fast changes in the spectra around half filling. We note, however, that these fast changes for the small cluster could be (partly) due to the finite size.

The two-pole approach completely neglects the width of the  $\vec{k}$ -dependent spectra since the entire LHB has collapsed into a single  $\delta$  peak for each value of  $\vec{k}$ . In the Appendix we give the expression for the  $\vec{k}$ -dependent second moment which determines the width. The  $k$ -dependent width of the LHB in one dimension is plotted in Fig. 16.

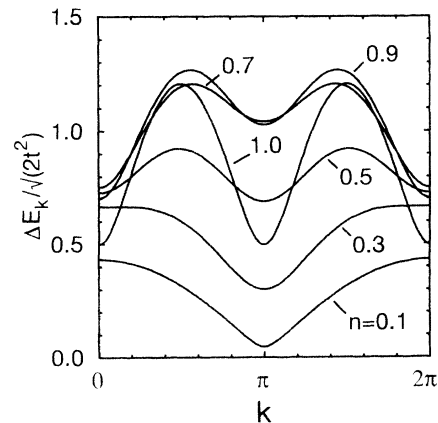


FIG. 16. Momentum dependence of the width of the lower band  $\Delta E_k / \sqrt{2t^2}$  in one dimension, for various fillings  $n$ .

At half filling the width is proportional to  $\cos(2k)$  and the maximal width is found at  $k = \pi/2$ . Here the width is  $\Delta E = \sqrt{6 \ln 2 - 9\zeta(3)/4} \times \sqrt{2}t^2$ , which is about 1.2 times as large as the  $k$ -integrated free-particle bandwidth.<sup>77,78</sup> The double period is lost away from half filling and the width increases compared to the half-filled case. The  $k$ -dependent spectra are still broad for densities  $n$  as small as 0.3. So even in the low-density case the incoherent spectral intensity is spread over a considerable energy range. Clearly the two-pole approach reproduces not more than just the average behavior of the energy in the Hubbard bands and does not account for the many-body effects, which lead to the broadening of the initial one-particle states.

## VII. SUMMARY AND CONCLUSIONS

In summary, following the paper by Harris and Lange,<sup>7</sup> we used the transformation from Hubbard to the strong-coupling model to derive expressions for various sum rules of the individual Hubbard bands. In one dimension the spin-charge decoupling for  $U = \infty$  enabled us to evaluate explicitly all quantities. The crucial point is that in order to get a good description of the spectra of the Hubbard model one should not only transform the Hamiltonian, but also all the relevant operators at the same time, such as the current operator for the optical spectrum and the creation operator for the one-particle spectrum. That also the operators become different is generally neglected or simply not realized. As we have shown this leads to large, in general first-order, corrections.

The above transformation is useful not only for the spectra, but also for evaluating static expectation values in the Hubbard model. In particular, when a nontrivial quantity in the Hubbard case becomes trivial in the strong-coupling model, this transformation produces explicit expressions. Examples are the  $\vec{k}$ -dependent occupation number at half filling and the amount of doubly occupied sites (potential energy).

For the optical spectrum sum rules were derived for the conductivity of the LHB and the UHB. The transformation of the total sum rule, the kinetic energy in the Hubbard model, leads to a first-order correction which is equal to the expectation value of the three-site hopping (including the nearest-neighbor spin expectation values). This correction term is dominant around half filling, where the kinetic energy of the Hubbard model is sizable due to the admixture of doubly occupied sites. The LHB and the UHB were shown to probe different parts of the three-site hopping correction. The UHB intensity is determined by the spin correlation function and the weight is therefore a direct measure of the (short-range) spin order. The weight of the LHB is enhanced by the three-site hopping to next neighbors of distance  $\sqrt{2}$  and 2. Apart from this there is a kinetic transfer of weight from the UHB to the LHB involving the next-nearest-neighbor hopping at distance 2.

In one dimension the Ogata-Shiba wave function<sup>35</sup> enabled us to obtain explicit expressions for the weights. Since in 1D the spin correlations are not weakened by

the holes, the decrease of the weight in the UHB with doping is given by counting the number of bonds between nearest-neighbor spins and is reduced further by the kinetic term  $W_U = (1 - 3x)W_U(n = 1)$ . This weight reduction is *six times faster* than expected for a simple semiconductor. In higher dimensions the spin order around the hole will become less antiferromagnetic, leading to an even faster disappearance of the UHB. In one dimension we have shown that the weight of the LHB is equal to the weight of the zero-frequency Drude peak to order  $t^3/U^2$ . This manifestation of spin-charge separation influences the entire LHB, but not the UHB. The excitations to the UHB, involving doubly occupied sites, is qualitatively independent of the dimension.

For the one-particle spectrum we derived expressions for the weight of the LHB and the UHB to second order. The zeroth-order term is easily understood by counting the available states for electron addition. The first- and second-order terms are both of a kinetic origin and both *enhance* the weight of the LHB close to half filling. These kinetic contributions are due to the constructive interference between the ground state and low-energy final states. We derived expressions of the weights for both the Hubbard and the strong-coupling model ground state. All expressions are explicitly electron-hole symmetric and vanish at half filling. The energy separation between the two bands to order  $t$  is  $U$  at half filling and increases to  $U + zt$  for  $n \rightarrow 0$ , where  $z$  is the number of neighbors. The width of the bands to order  $t$  is equal to the free-particle width at half filling. Away from half filling the UHB narrows and its width goes to zero for  $n \rightarrow 0$ . The LHB becomes broader with increasing  $x$ .

The  $\vec{k}$  dependence of the spectral moments of the individual bands is studied using both perturbation theory and the related two-pole ansatz. A comparison of both methods shows that the two poles can be identified with the two Hubbard bands only to first order in  $t/U$ . The general result is that the  $\vec{k}$  dependence of the spectra around half filling is determined for a large part by the spin order. For very large  $U$  the average energy of the LHB has a normal cosine dispersion for paramagnetic or ferromagnetic spin correlations, but has a reversed  $-\cos(k)$  dispersion close to half filling and for nearest-neighbor spin correlations smaller than  $-1/4$  (Néel order). For intermediate  $U$  the two-pole approach gives a much better description of the fast density-dependent changes around half filling in the  $\vec{k}$ -dependent spectra than the perturbation theory. However, the often neglected  $\vec{k}$ -dependent terms in the two-pole approach are essential to get the correct behavior. The expressions for the  $\vec{k}$ -dependent second moment show that the spectra are very incoherent and that the incoherent width for certain  $\vec{k}$  values is often larger than the total  $\vec{k}$ -integrated width of the LHB.

The distribution of weight over the two Hubbard bands, in both the one-particle and the optical spectra, is qualitatively independent of the dimension and whether or not there is spin-charge separation. This is a manifestation of the fact that the sum rules are determined locally and depend on nearest- and next-nearest-

neighbor expectation values only. On the contrary, the current operator in the optical spectrum probes only the charge part and therefore the conductivity in the LHB is completely different in one dimension as compared to two dimensions. In both spectroscopies the features observed are strongly influenced by the local spin correlations. The three-site hopping contributions are crucial to understand the observed strong doping-dependent intensity changes and demonstrate the importance of these processes in the Hubbard model. In the  $t$ - $J$  model only the backward hopping  $\sim \vec{S}_i \cdot \vec{S}_{i+\delta}$  of the three-site hopping is kept in the Hamiltonian. For the optical spectrum the neglect of the next-neighbor hopping processes in the Hamiltonian results also in the neglect of the respective contributions of these processes to the weights of the LHB and the UHB. Therefore, the  $t$ - $J$  model does *not* represent the spectral properties of the Hubbard model for intermediate or even large  $U$ . Furthermore, we note that also the transport properties of the strong-coupling and the  $t$ - $J$  model are quite different and the superconducting order parameter exhibits a different  $\vec{k}$  dependence of the gap in both models.<sup>80</sup>

Because of the local character of the sum rules the agreement between the perturbation expressions for the infinite system and the numerical finite-size cluster results is quite good for large  $U$ . For  $U$  of the order of the bandwidth the perturbation expressions still describe the qualitative changes, but quantitatively errors of roughly 30% occur due to the neglect of higher-order terms.

The oxygen  $1s$  electron-energy-loss experiments as well as the measured optical conductivity show an anomalously fast decrease of the intensity of the UHB with doping. We have shown that this effect is a natural consequence of the strong correlations in these materials and can be understood easily starting from an ionic picture with two Hubbard bands. As such the observation of fast weight changes is a fingerprint of systems with a (Hubbard) gap caused by electron correlations. We stress that, although this weight transfer is observed in both experiments, the interpretation in both cases is quite different. In the optical spectrum the nearest-neighbor spin order is involved, while in the one-particle case the lowest-order effect is understood by counting the available degrees of freedom to add a particle to a particular site. Of course this phenomenon is not restricted to the cuprate mate-

rials, but similar effects have already been observed in hole-doped  $\text{La}_2\text{NiO}_4$  (Ref. 6) and are expected in any compound with an effective on-site repulsion bigger than or of the order of the band width. This is expected to be the case in some realistic situations, where the multiband models do not necessarily map onto the one-band Hubbard model and one is left with a more complex model as, for instance, in the late transition-metal oxides. In fact, even more dramatic transfers of the spectral weight might be present in such models due to the competition between the kinetic and magnetic energies at finite doping which promotes magnetically ordered states other than those found in the undoped Mott-Hubbard insulators.<sup>81</sup> Also, if one introduces orbital degeneracy in the Hubbard model, the effects are much more dramatic. In this case the total intensity of the Hubbard bands is proportional to  $2N_a d$ , where  $d$  is the orbital degeneracy.<sup>82</sup> If one removes only one electron by doping, starting from a particular integer filling with  $n$  electrons per unit cell, then there are  $2d - (n - 1)$  ways to put one electron in the LHB in inverse photoemission, which is (in general) larger than the factor 2 in the single-band model.

#### ACKNOWLEDGMENTS

We thank P. Horsch, G. A. Sawatzky, B. Mehlig, V. Zevin, and especially L. F. Feiner for very stimulating discussions. One of us (A.M.O.) acknowledges the financial support by the Committee of Scientific Research (KBN) of Poland, Project No. 2 P302 93 055 05.

#### APPENDIX

The simplest estimation of the width of the LHB is provided by the  $\vec{k}$ -dependent second moment

$$m_{\vec{k};0}^{(2)} = \frac{1}{N_a} \sum_{i,j,\sigma} e^{i\vec{k}\cdot(\vec{R}_i - \vec{R}_j)} \left\langle \left\{ [a_{i,\sigma;0}, H], [H, a_{j,\sigma;0}^\dagger] \right\} \right\rangle. \quad (\text{A1})$$

In lowest order it is simplified to

$$m_{\vec{k};0}^{(2)} = \frac{1}{N_a} \sum_{i,j,\sigma} e^{i\vec{k}\cdot(\vec{R}_i - \vec{R}_j)} \times \left\langle \left\{ [c_{i,\sigma;0}, \tilde{T}_0], [\tilde{T}_0, c_{j,\sigma;0}^\dagger] \right\} \right\rangle + \mathcal{O}(t^3/U). \quad (\text{A2})$$

Using Eq. (9) this is related to the two- and three-site correlation functions as

$$\begin{aligned} m_{\vec{k};0}^{(2)} &= zt^2(2-n) - \frac{t^2}{N_a} \sum_{i,\delta,\delta',\sigma;\delta\neq\delta'} \left\langle c_{i+\delta,\sigma}^\dagger \tilde{n}_i c_{i+\delta',\sigma} - 2(c_{i+\delta,\sigma}^\dagger \tilde{n}_i \tilde{\sigma} c_{i+\delta',\sigma} - c_{i+\delta,\sigma}^\dagger c_{i,\tilde{\sigma}}^\dagger c_{i,\sigma} c_{i+\delta',\tilde{\sigma}}) \right\rangle \\ &+ 2t\epsilon_{\vec{k}} \frac{z-1}{zN_a} \sum_{i,\delta,\sigma} \left\langle c_{i,\sigma}^\dagger c_{i+\delta,\sigma} \right\rangle - 2t\epsilon_{\vec{k}} \frac{1}{zN_a} \sum_{i,\delta,\delta',\sigma;\delta\neq\delta'} \left\langle \tilde{n}_{i+\delta,\sigma} c_{i+\delta',\sigma}^\dagger c_{i,\sigma} + c_{i+\delta',\sigma}^\dagger c_{i+\delta,\tilde{\sigma}}^\dagger c_{i+\delta,\sigma} c_{i,\tilde{\sigma}} \right\rangle \\ &+ \frac{t^2}{N_a} \sum_{i,\delta,\delta',\sigma;\delta\neq\delta'} e^{i\vec{k}\cdot(\vec{\delta}' - \vec{\delta})} \left\langle 1 - \frac{3}{2}n + \frac{1}{4}\tilde{n}_i \tilde{n}_{i+\delta} \tilde{n}_{i+\delta'} + (2 - \tilde{n}_{i+\delta'}) \left( \tilde{n}_{i,\sigma} \tilde{n}_{i+\delta,\sigma} + c_{i+\delta,\tilde{\sigma}}^\dagger c_{i,\sigma}^\dagger c_{i,\tilde{\sigma}} c_{i+\delta,\sigma} \right) \right. \\ &\left. + \left( 1 - \frac{\tilde{n}_i}{2} \right) \left( \tilde{n}_{i+\delta,\sigma} \tilde{n}_{i+\delta',\sigma} + c_{i+\delta,\tilde{\sigma}}^\dagger c_{i+\delta',\sigma}^\dagger c_{i+\delta',\tilde{\sigma}} c_{i+\delta,\sigma} \right) \right\rangle. \quad (\text{A3}) \end{aligned}$$

At half filling ( $n = 1$ ) all summations vanish, except the last one. Therefore the  $\vec{k}$ -dependent part of the second moment is proportional to  $\cos(2k)$ . The last term now contains nearest-neighbor and next-nearest-neighbor correlation functions. For an antiferromagnetic spin order the second moment becomes  $\vec{k}$  independent.<sup>62</sup>

The above equation can again be solved in 1D by means of the Ogata-Shiba wave function.<sup>35</sup> In this case we need also the next-nearest-neighbor spin-spin correlation function for the Heisenberg chain, which has been obtained by Takahashi.<sup>32</sup> The final result in one dimension is

$$\begin{aligned}
m_{k;0}^{(2),1D} = & 2t^2(2-n) - 2t^2(1+2\ln 2) \left[ n \frac{\sin(2\pi n)}{2\pi} - \frac{\sin^2(\pi n)}{\pi^2} \right] - 4t^2 \cos(k) \frac{\sin(\pi n)}{\pi} \left\{ 1 - (1-2\ln 2) \left[ n - \frac{\sin(2\pi n)}{2\pi} \right] \right\} \\
& + 2t^2 \cos(2k) \left\{ 2 - 3n + (1-2\ln 2) \left[ 3n^2 - 2 \frac{\sin^2(\pi n)}{\pi^2} - \frac{\sin^2(2\pi n)}{(2\pi)^2} \right] \right. \\
& \left. + \left( \frac{9}{4} \zeta(3) - 1 \right) \left[ n^3 - 2n \frac{\sin^2(\pi n)}{\pi^2} - n \frac{\sin^2(2\pi n)}{(2\pi)^2} + 2 \frac{\sin(2\pi n)}{2\pi} \frac{\sin^2(\pi n)}{\pi^2} \right] \right\}. \tag{A4}
\end{aligned}$$

Here  $\zeta(z)$  is the Riemann zeta function. The width of the LHB is now defined as

$$(\Delta E_k^{\text{LHB},1D})^2 = \frac{m_{k;0}^{(2),1D}}{m_{k;0}^{(0),1D}} - \left( \frac{m_{k;0}^{(1),1D}}{m_{k;0}^{(0),1D}} \right)^2, \tag{A5}$$

where the first moment was calculated before [Eq. (82)] and the zeroth moment is equal to  $2-n$  to lowest order.

- 
- <sup>1</sup> H. Romberg, M. Alexander, N. Nücker, P. Adelman, and J. Fink, Phys. Rev. B **42**, 8768 (1990).  
<sup>2</sup> C. T. Chen *et al.*, Phys. Rev. Lett. **66**, 104 (1991).  
<sup>3</sup> P. Kuiper *et al.*, Phys. Rev. Lett. **62**, 221 (1989).  
<sup>4</sup> S. L. Cooper *et al.*, Phys. Rev. B **41**, 11605 (1990); **45**, 2549 (1992).  
<sup>5</sup> S. Uchida, T. Ido, H. Takagi, T. Arima, Y. Tokura, and S. Tajima, Phys. Rev. B **43**, 7942 (1991).  
<sup>6</sup> T. Ido *et al.*, Phys. Rev. B **44**, 12094 (1991).  
<sup>7</sup> A. B. Harris and R. V. Lange, Phys. Rev. **157**, 295 (1967).  
<sup>8</sup> H. Eskes, M. B. J. Meinders, and G. A. Sawatzky, Phys. Rev. Lett. **67**, 1035 (1991).  
<sup>9</sup> M. S. Hybertsen, E. B. Stechel, W. M. C. Foulkes, and M. Schlüter, Phys. Rev. B **45**, 10032 (1992).  
<sup>10</sup> Y. Ohta, K. Tsutsui, W. Koshibae, T. Shmozato, and S. Maekawa, Phys. Rev. B **46**, 14022 (1992).  
<sup>11</sup> M. B. J. Meinders, H. Eskes, and G. A. Sawatzky, Phys. Rev. B **48**, 3916 (1993).  
<sup>12</sup> P. Horsch *et al.*, Physica C **162-164**, 783 (1989); H. Eskes and G. A. Sawatzky, in *Electronic Properties of High-T<sub>c</sub> Superconductors and Related Compounds*, edited by H. Kuzmany, M. Mehring, and J. Fink, Springer Series in Solid-State Sciences Vol. 99 (Springer-Verlag, Berlin, 1990), p. 127; H. J. Schmidt and Y. Kuramoto, Phys. Rev. B **42**, 2562 (1990); H. Eskes and G. A. Sawatzky, *ibid.* **43**, 119 (1991); G. Dopf *et al.*, Phys. Rev. Lett. **68**, 2082 (1992); E. Dagotto, F. Ortolani, and D. Scalapino, *ibid.* **46**, 3183 (1992); G. S. Feng and S. R. White, Phys. Rev. B **46**, 8691 (1992); P. W. Leung *et al.*, *ibid.* **46**, 11779 (1992); N. Bulut, D. J. Scalapino, and S. R. White, Phys. Rev. Lett. **72**, 705 (1994); R. Preuss, A. Muramatsu, W. von der Linden, F. F. Assaad, and W. Hanke, *ibid.* **73**, 732 (1994).  
<sup>13</sup> A. Moreo and E. Dagotto, Phys. Rev. B **42**, 4786 (1990); W. Stephan and P. Horsch, *ibid.* **42**, 8736 (1990); T. Toyama and S. Maekawa, Physica C **185-189**, 1575 (1991); J. Wagner, W. Hanke, and D. J. Scalapino, Phys. Rev. B **43**, 10517 (1991); E. Dagotto *et al.*, *ibid.* **45**, 10107 (1992).  
<sup>14</sup> P. Unger and P. Fulde, Phys. Rev. B **47**, 8947 (1993); **48**, 16607 (1993).  
<sup>15</sup> R. Hayn, V. Yushankhai, and S. Lovtsov, Phys. Rev. B **47**, 5253 (1993).  
<sup>16</sup> J. Zaanen, G. A. Sawatzky, and J. W. Allen, Phys. Rev. Lett. **55**, 418 (1985).  
<sup>17</sup> F. C. Zhang and T. M. Rice, Phys. Rev. B **37**, 3759 (1988).  
<sup>18</sup> H. Eskes and G. A. Sawatzky, Phys. Rev. Lett. **61**, 1415 (1988).  
<sup>19</sup> M. S. Hybertsen, E. B. Stechel, M. Schlüter, and D. R. Jennison, Phys. Rev. B **41**, 11068 (1990).  
<sup>20</sup> S. B. Bacci, E. R. Gagliano, R. M. Martin, and J. F. Annett, Phys. Rev. B **44**, 7504 (1991).  
<sup>21</sup> S. V. Lovtsov and V. Y. Yushankhai, Physica C **179**, 159 (1991).  
<sup>22</sup> J. H. Jefferson, H. Eskes, and L. F. Feiner, Phys. Rev. B **45**, 7959 (1992).  
<sup>23</sup> H. B. Schüttler and A. J. Fedro, Phys. Rev. B **45**, 7588 (1992).  
<sup>24</sup> V. I. Belinicher and A. L. Chernyshev, Phys. Rev. B **49**, 9746 (1994).  
<sup>25</sup> L. F. Feiner, J. H. Jefferson, and R. Raimondi (unpublished).  
<sup>26</sup> L. F. Feiner, Phys. Rev. B **48**, 16857 (1993).  
<sup>27</sup> J. Hubbard, Proc. R. Soc. London, Ser. A **276**, 238 (1963).  
<sup>28</sup> P. W. Anderson, Phys. Rev. **115**, 2 (1959).  
<sup>29</sup> L. N. Bulaevskii, Zh. Eksp. Teor. Fiz. **51**, 230 (1966) [Sov. Phys. JETP **24**, 154 (1967)].  
<sup>30</sup> D. J. Klein and W. A. Seitz, Phys. Rev. B **8**, 2236 (1973).  
<sup>31</sup> K. A. Chao, J. Spałek, and A. M. Oleś, J. Phys. C **10**, L271 (1977); Phys. Rev. B **18**, 3453 (1978).  
<sup>32</sup> M. Takahashi, J. Phys. C **10**, 1289 (1977).  
<sup>33</sup> A. H. MacDonald, S. M. Girvin, and D. Yoshioka, Phys. Rev. B **37**, 9753 (1988).  
<sup>34</sup> H. Shiba, Phys. Rev. B **6**, 930 (1972).  
<sup>35</sup> M. Ogata and H. Shiba, Phys. Rev. B **41**, 2326 (1990).  
<sup>36</sup> G. D. Mahan, *Many Particle Physics* (Plenum Press, New York, 1981), Chap. 1.  
<sup>37</sup> For a finite system with periodic boundary conditions the total weight distributes over a finite frequency part and a zero frequency Drude peak and Eq. (34) cannot be used. Instead, the sum rule for the UHB to lowest order can be derived directly from Eq. (33) without using the polarization. Approximating  $1/\omega$  by  $1/U$ , this sum rule is propor-

- tional to  $\langle j_{\mathbf{x};-Uj_{\mathbf{x};U} \rangle$ , the evaluation of which gives again Eq. (41). Since the total sum rule  $W$  is the kinetic energy for both types of boundaries, Eqs. (38) and (39) follow.
- <sup>38</sup> W. Kohn, Phys. Rev. **133**, A171 (1964).
- <sup>39</sup> P. F. Maldague, Phys. Rev. B **16**, 2437 (1977).
- <sup>40</sup> B. S. Shastry and B. Sutherland, Phys. Rev. Lett. **65**, 243 (1990).
- <sup>41</sup> A. J. Millis and S. N. Coppersmith, Phys. Rev. B **42**, 10 807 (1990).
- <sup>42</sup> D. Baeriswyl, J. Carmelo, and A. Luther, Phys. Rev. B **33**, 7247 (1986).
- <sup>43</sup> H. J. Schulz, Int. J. Mod. Phys. B **5**, 57 (1991).
- <sup>44</sup> J. Carmelo, P. Horsch, P. A. Bares, and A. A. Ovchinnikov, Phys. Rev. B **44**, 9967 (1991).
- <sup>45</sup> P. Horsch and W. Stephan, Phys. Rev. B **48**, 10 595 (1993).
- <sup>46</sup> M. Ogata, T. Sugiyama, and H. Shiba, Phys. Rev. B **43**, 8401 (1991).
- <sup>47</sup> R. B. Griffiths, Phys. Rev. **133**, A768 (1964).
- <sup>48</sup> Y. Endoh, G. Shirane, R. J. Birgeneau, P. M. Richards, and S. L. Holt, Phys. Rev. Lett. **32**, 170 (1974).
- <sup>49</sup> W. Stephan and P. Horsch, Int. J. Mod. Phys. B **6**, 141 (1992).
- <sup>50</sup> J. Lorenzana and L. Yu, Phys. Rev. Lett. **70**, 861 (1993).
- <sup>51</sup> R. M. Fye, M. J. Martins, D. J. Scalapino, J. Wagner, and W. Hanke, Phys. Rev. B **44**, 6909 (1991).
- <sup>52</sup> L. Roth, Phys. Rev. **184**, 451 (1969).
- <sup>53</sup> C. Castellani *et al.*, Phys. Rev. Lett. **69**, 2009 (1992); R. Raimondi and C. Castellani, Phys. Rev. B **48**, 11 453 (1993).
- <sup>54</sup> G. Beni, T. Holstein, and P. Pincus, Phys. Rev. B **8**, 312 (1973).
- <sup>55</sup> A. M. Oleś, G. Tréglia, D. Spanjaard, and R. Jullien, Phys. Rev. B **34**, 5101 (1986).
- <sup>56</sup> J. B. Grant and A. K. McMahan, Phys. Rev. B **46**, 8440 (1992).
- <sup>57</sup> M. P. López Sancho, J. Rubio, M. C. Refolio, and J. M. López Sancho, Phys. Rev. B **46**, 11 110 (1992).
- <sup>58</sup> O. Gunnarsson and K. Schönhammer, Phys. Rev. B **28**, 4315 (1983).
- <sup>59</sup> C. Lehner, G. Baumgärtel, J. Schmalian, and K.-H. Bennemann, Solid State Commun. **89**, 719 (1994).
- <sup>60</sup> H. Eskes, Ph. D. thesis, University of Groningen, The Netherlands, 1992.
- <sup>61</sup> G. A. Sawatzky, Phys. Rev. Lett. **39**, 504 (1977).
- <sup>62</sup> W. F. Brinkman and T. M. Rice, Phys. Rev. B **2**, 1324 (1970).
- <sup>63</sup> W. Nolting, Z. Phys. B **265**, 173 (1973).
- <sup>64</sup> G. Geipel and W. Nolting, Phys. Rev. B **38**, 2608 (1988).
- <sup>65</sup> W. Nolting and W. Borgiel, Phys. Rev. B **39**, 6962 (1989); W. Nolting, W. Borgiel, V. Dose, and T. Fauster, *ibid.* **40**, 5015 (1989).
- <sup>66</sup> B. Mehlig, H. Eskes, R. Hayn, and M. B. J. Meinders (unpublished).
- <sup>67</sup> D. M. Esterling and R. V. Lange, Rev. Mod. Phys. **40**, 796 (1968).
- <sup>68</sup> O. K. Kalashnikov and E. D. Fradkin, Phys. Status Solidi B **59**, 9 (1973).
- <sup>69</sup> E. G. Goryachev, E. V. Kuzmin, and S. G. Ovchinnikov, J. Phys. C **15**, 1481 (1982).
- <sup>70</sup> L. S. Campana *et al.*, Physica A **123**, 279 (1984); Phys. Rev. B **30**, 2769 (1984).
- <sup>71</sup> W. Nolting and A. M. Oleś, Physica A **143**, 296 (1987).
- <sup>72</sup> A. E. Ruckenstein and S. Schmitt-Rink, Int. J. Mod. Phys. B **3**, 1809 (1989).
- <sup>73</sup> Y. Zhou *et al.*, Phys. Rev. B **44**, 10 291 (1991).
- <sup>74</sup> A. M. Oleś, G. Tréglia, D. Spanjaard, and R. Jullien, Phys. Rev. B **32**, 2167 (1985).
- <sup>75</sup> K. J. von Szczepanski, P. Horsch, W. Stephan, and M. Ziegler, Phys. Rev. B **41**, 2017 (1990).
- <sup>76</sup> W. Stephan and P. Horsch, Phys. Rev. Lett. **66**, 2258 (1991).
- <sup>77</sup> M. Ziegler and P. Horsch, in *Dynamics of Magnetic Fluctuations in High-Temperature Superconductors*, edited by G. Reiter, P. Horsch and G. Psaltakis (Plenum Press, New York, 1991), p. 329.
- <sup>78</sup> S. Sorella and A. Parola, J. Phys. Condens. Matter **4**, 3589 (1992).
- <sup>79</sup> C. L. Kane, P. A. Lee, and N. Read, Phys. Rev. B **39**, 6880 (1989).
- <sup>80</sup> J. Spalek, Phys. Rev. B **40**, 5180 (1989); K. Byczuk and J. Spalek, Acta Phys. Polon. A **85**, 337 (1994).
- <sup>81</sup> J. Zaanen and A. M. Oleś, Phys. Rev. B **47**, 7197 (1993).
- <sup>82</sup> M. B. J. Meinders, Ph. D. thesis, University of Groningen, The Netherlands, 1994.